Russian Chemical Reviews **80** (12) 1191 – 1207 (2011) © 2011 Russian Academy of Sciences and Turpion Ltd

DOI 10.1070/RC2011v080n12ABEH004237

Photonic crystals based on opals and inverse opals: synthesis and structural features

S O Klimonsky, V V Abramova, A S Sinitskii, Yu D Tretyakov

Contents

I.	Introduction	1191
II.	Photonic crystals and photonic band gaps	1191
III.	The synthesis of opals and inverse opals	1193
IV.	Structural features of opals and inverse opals	1197
V.	Methods of investigation of structural defects in opals and inverse opals	1199
VI.	Conclusion	1203

Abstract. Methods of synthesis of photonic crystals based on opals and inverse opals are considered. Their structural features are discussed. Data on different types of structural defects and their influence on the optical properties of opaline materials are systematized. The possibilities of investigation of structural defects by optical spectroscopy, electron microscopy, microradian X-ray diffraction, laser diffraction and using an analysis of Kossel ring patterns are described. The bibliography includes 253 references.

I. Introduction

Photonic crystals, as structural units for control of light flow, have a great potential for application in photonic techniques. The first observation of a photonic band gap in synthetic opals (photonic crystalline materials with the opal and inverse opal structures) was reported in 1995.[1] Since then, considerable attention has been paid to such materials. Their advantages include a relative simplicity of synthetic routes and the lack of limitations on the sample size. A main drawback is the presence of natural structural defects appearing during the synthesis.

Unlike other reviews devoted to the investigations of this type of photonic crystals,[2–6] in the present study the emphasis is placed on structural features of opals and inverse opals and on the corresponding methods of investigation.

S O Klimonsky, V V Abramova, A S Sinitskii, Yu D Tretyakov Department of Materials Science and Department of Chemistry, M V Lomonosov Moscow State University, Leninskie Gory 1, 119991 Moscow, Russian Federation. Fax (7-495) 939 09 98, tel. (7-495) 939 20 74, e-mail: klim@inorg.chem.msu.ru (S O Klimonsky), abramova.vera@gmail.com (V V Abramova), sinitskii@gmail.com (A S Sinitskii), tel. (7-495) 939 20 74, e-mail: yudt@inorg.chem.msu.ru (Yu D Tretyakov)

Received 12 October 2011
Uspekhi Khimii **80** (12) 1244 – 1262 (2011); translated by A M Raevskiy

II. Photonic crystals and photonic band gaps

The scope of the science of photonics includes the principles of design of devices whose operation is based on various photon-related phenomena. Progress in photonics can lead to a breakthrough in data transfer and information processing technologies.[2] Studies in this field began with the invention of lasers and optical fibres that act as sources of and transmission lines for the new type of information carriers, *viz*., photons. However, further development of photonics requires the design and fabrication of logical devices for manipulation of signals. Possible candidates for such devices are the so-called photonic crystals, *i.e*., materials characterized by spatially-periodic changes in the refractive index on the length scale of the wavelengths of certain types of electromagnetic radiation. Note that the term 'crystals' is only formally applicable to these materials because they consist of the same structural units whose size is much larger than the size of an atom, being comparable with the wavelengths of electromagnetic radiation in the visible or IR regions. Nevertheless, the term 'photonic crystals' is commonly recognized at present because of numerous analogies between the photonic and conventional (atomic) crystals. All crystals including atomic, ionic, molecular ones, *etc*. effectively scatter some types of radiation (X-ray radiation, neutron radiation, *etc*.) provided that the lattice constants are of the same order of magnitude as the radiation wavelength. Photonic crystals can also be transparent to a broad spectrum of electromagnetic radiation; however, they do not transmit light with the wavelengths comparable with the lattice constant. Due to the Bragg diffraction the energy spectrum of photons is divided into the allowed and forbidden bands similarly to the case for electronic spectra of conventional crystals.

Intensive research on photonic crystals began in 1987 when fundamental theoretical studies by Yablonovitch[7] and John[8] were reported. Yablonovitch[7] proposed to use structures with periodic modulation of the refractive index for controlling the probability of spontaneous emission. John[8] considered localization of light in analogous struc-

tures with artificial defects. However, it should be noted that many fundamental ideas indissolubly related to photonic crystals were for the first time reported much earlier, namely, in Bykov's studies,[9–11] which for long did not draw attention of research community. Bykov theoretically investigated spontaneous emission of atoms and molecules placed in a model one-dimensional (1D) photonic crystal whose photonic band gap corresponded to the wavelength of emitted photons. According to calculations, if the number of layers in photonic crystals is sufficiently large, spontaneous emission can be almost completely suppressed. Based on the results obtained, Bykov was the first who proposed to use the effect of suppression of spontaneous emission for fabrication of low-threshold lasers. To this end, he proposed to use three-dimensional (3D) photonic crystals characterized by only one direction of propagation of radiation, all other directions being suppressed. More recently, the idea of using 3D photonic crystals to suppress spontaneous emission was repeated by Yablonovitch.[7] Interestingly, studies[9–11] were published long before the term 'photonic crystal' was coined; Bykov called the structures he investigated 'periodic media with band energy spectrum'.

Depending on the structure and on the ratio of the dielectric constants of the dielectrics forming a photonic crystal, it can have a complete band gap, a pseudo-band gap or a stop band. The presence of a complete bandgap means that in some spectral region, electromagnetic waves of any polarization cannot enter the crystal or go out along any crystallographic direction. As an example, Fig. 1 presents the photonic band structure of a photonic crystal formed by hollow silica spheres packed into a face-centred cubic (fcc) lattice.[12] As can be seen, a complete photonic band gap is observed at $\omega a/(2\pi c) \approx 0.83$, where ω is the angular frequency, a is the lattice constant of the cubic photonic crystal and c is the speed of light in vacuum. A feature of a pseudo-band gap is that the impossibility condition for electromagnetic waves from a particular spectral region to enter a crystal or to go out is violated along some direction (or directions), *i.e.*, the complete photonic band gap is collapsed along this direction (directions). A 'stop band' is a wavelength range for which propagation along a particular crystallographic direction is forbidden. For example, Fig. 1,*a* demonstrates a stop band at $0.45 < \omega a/(2\pi c) < 0.54$ for the ΓL direction. Three-dimensional photonic crystals can have a complete band gap, a pseudo-band gap and always have a number of stop bands. Two-dimensional (2D) and 1D photonic crystals only have the stop bands.

Fields of application of photonic crystals can be related to either the existence of a complete photonic band gap or some features of dispersion of the available bands.[2] For instance, forbiddenness of propagation of light along undesired directions could solve the problem of the design of highly efficient light-emitting diodes.[13,14] Creation of artificial defects in photonic crystals with a complete photonic band gap offers additional prospects for control of light flow including fabrication of light guides configured in any way.[15–18] Microcavities in 2D photonic crystals can serve as a basis for engineering low-threshold lasers.[19,20] Other variants of creation of sources of stimulated emission based on photonic crystals can be related to lasing due to optical feedback owing to Bragg reflection in the region of photonic band gap, lasing with distributed feedback in a

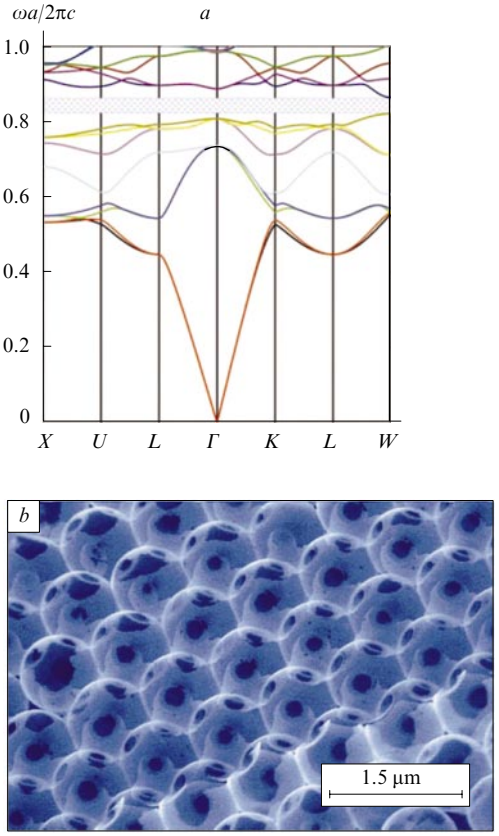


Figure 1. Energy band structure of a photonic crystal formed by hollow silica spheres packed in the fcc lattice (*a*) and an electron micrograph of the corresponding photonic crystal (*b*).[12]

periodic structure as well as (as applied to opal-like structures) lasing in a highly scattering medium.[21–23] Lasing can also be favoured by an extended flat portion with a nearly-zero group velocity at the boundary of the allowed photonic band.[2,3,24,25] These portions can be of considerable importance for enhancement of various (*e.g.*, magneto-optical, nonlinear optical, photocatalytic) effects due to the interaction of light with matter,[3,5] fabrication of delay lines, phase shifters and amplifiers. Inoue *et al.*[26,27] theoretically and experimentally studied the amplification of magneto-optical effects in 1D photonic crystals due to light concentration in the magnetic layer. Enhancement of the Kerr effect was achieved due to generation of the surface plasmon-polariton waves in 1D conducting photonic crystals.[28,29] It was also observed for 3D photonic crystals based on opal with (i) yttrium iron garnet[30] and (ii) magnetite[31] as well as nickel inverse opals.[32] Abnormal dispersion of opal-like polystyrene photonic crystals was used for enhancement of the third harmonic generation.[33] More recently, photonic crystals of composite materials based on opals were also used to enhance the second harmonic generation.[34] Abrupt acceleration of photocatalytic degradation of a dye inside inverse TiO_2 was demonstrated experimentally.[35] Specific features of dispersion laws also govern the applications of photonic crystals as superprisms,[36] superlenses[37] and for control of the radiation pattern of luminescent photonic crystals.[38–43]

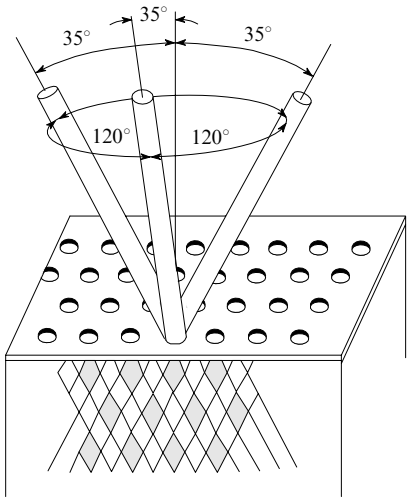


Figure 2. Fabrication of photonic crystals by drilling an ordered array of openings in a dielectric material: a schematic.[44]

The first three-dimensional photonic crystal was obtained and investigated by Yablonovitch *et al.*[44] Cylindrical openings were drilled in a dielectric material in such a manner that a fcc lattice of voids was formed in the bulk of the material (Fig. 2). According to experimental data, the structure thus obtained had a complete band gap in the microwave region. It was emphasized[44] that analogous structures with submicrometer periodicity can probably be obtained by ion etching of Si or GaAs, which should lead to the formation of photonic crystals with a complete photonic band gap in the visible and near-IR regions. Indeed, such photonic crystals for the IR region were reported nearly a decade ago.[12,45,46] The conditions that should be met to obtain a complete photonic band gap were established. First of all, it was found that the symmetry considerations and degeneration of the allowed bands at the W and U points of the Brillouin zones prevent fcc crystals composed of colloidal spheres (synthetic opals) from having a complete photonic band gap at all.[47] At the same time, a complete photonic band gap (between the eighth and ninth allowed bands) can be opened in the so-called inverse opals whose structures comprise spheres with a low refractive index n_1 (*e.g.*, air voids) distributed within a matrix with a higher refractive index (n_2) provided that the ratio n_2/n_1 called the optical contrast of a structure exceeds a value of 2.8.[48,49] Silicon, germanium and some other semiconductor materials are characterized by appropriate n_2 values; however, these materials are opaque in the visible region. According to calculations,[50] a complete photonic band gap in a diamond-like structure is opened at an optical contrast of higher than two, but fabrication of such a structure from rather high-index materials faces significant difficulties.[51] As a result, the problem of obtaining photonic crystals with a complete band gap in the visible region is still to be solved.

To date, a large number of fundamentally different methods for fabrication of 2D and 3D photonic crystals with specified dielectric properties and spatial symmetry have been developed (see reviews[2–6,13]). In most cases, they can conditionally be treated as lithographic techniques (including laser printing and interference lithography) or methods based on self-assembly of monodisperse colloidal microparticles. Each group of methods has its advantages and drawbacks. Lithography allows one to synthesize almost perfect photonic crystals of different structure. However, a layer-by-layer buildup of a 3D lithographic structure takes a too long time (only a microscopic photonic crystal comprising a limited number of layers can be grown during an admissible period of time). This problem can to some extent be solved using interference lithography (or holographic lithography)[52] which is successfully used not only for the synthesis of simple photonic crystals, but also structures with artificial defects[53,54] and more exotic systems with periodic distribution of absorption centres promising for fabrication of fast optical switches.[55] However, the method has fundamental limitations on the engineering of structures with small (submicrometer) periodicity for the visible region, which is due to the wavelength of the laser used. At the same time, the methods based on self-assembly of colloidal microparticles require relatively simple equipment. They have no fundamental limitations on both the number of samples synthesized at once and their linear dimensions, and allow one to obtain with ease 3D photonic crystals with submicrometer periodicity of the structure. The main drawback of these techniques is unavoidable formation of structural defects.

III. The synthesis of opals and inverse opals

1. Synthesis of colloidal crystals

Close-packed structures forming by self-assembly of colloidal microparticles are called colloidal crystals or synthetic opals. Natural opals whose name was taken for the colloidal crystals also consist of close-packed microparticles (mainly silica hydrogel $SiO_2 \cdot x\,H_2O$ with variable content of water) 150–400 nm in diameter. Different modifications of natural opals may contain a variety of impurities, *viz.*, Al_2O_3 (to 9%), Fe_2O_3 (to 3%), TiO_2 (to 5%); sometimes, organic impurities are present. Natural opals are very brittle[56] and characterized by a Moos hardness in the range from 5.5 to 6, refractive indices from 1.44 to 1.46 and densities lying between 1.8 and 2.3 g cm^{-3}. Opals became widely known due to iridescence, an unusual trick of the light due to diffraction of light on the periodic structure formed by spherical microparticles.[57]

Synthetic opals based on SiO_2 microspheres are the closest to natural opals. They were for the first time obtained in the 1960s.[58] Synthetic opals are much like natural ones and characterized by a density of 2.03 g cm^{-3}, a refractive index of 1.44 and a Moos hardness of 4.5 (a somewhat lower value compared to natural opal). Synthetic opals were produced in the Soviet Union.[59] At present, they are grown in a few private companies in the Russian Federation, the USA, China and some other countries. In addition, various materials demonstrating a trick of the light characteristic of opals (*e.g.*, 'opals' obtained according to Slocum and representing pieces of glass with microscopic inhomogeneities and air bubbles) are now available on the jewelry market.

Fabrication of synthetic opals involves some stages.[59] First, the Stöber method[60] is used to synthesize a suspension of monodisperse amorphous SiO_2 spherical particles with average diameters in the range 200–800 nm. The method is essentially a hydrolysis of tetraethoxysilane $Si(OEt)_4$ (TEOS) in aqueous alcohol in the presence of ammonia as catalyst. The sizes of microparticles formed

depend on the concentrations of all components of the reaction mixture (TEOS, water, ammonia). The syntheses of monodisperse particles based on SiO_2 and polystyrene were considered in Refs 61–66 and in Refs 67–71, respectively.

Next, an aqueous suspension of SiO_2 microspheres is allowed to stay in a trough for a long time. Under the action of gravitational force, sedimentation occurs and particles form a periodic structure of hexagonally close-packed layers. The sediment is dried and then sintered at high temperature (usually, at least at 800 °C) to make the sample more dense and harder. Colloidal crystals based on polymeric microparticles can be obtained analogously; such samples are annealed at a much lower temperature (Fig. 3).

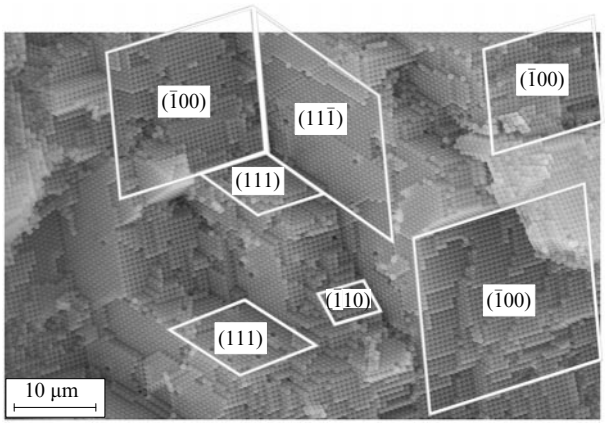


Figure 3. Electron micrograph of a colloidal crystal based on polystyrene microparticles obtained by sedimentation.
Shown are the crystallographic planes characteristic of the fcc structure.

Sedimentation of colloidal particles simulates the natural mechanism of formation of natural opal; therefore, it has long been studied.[56, 59] Long-term settling of suspension of colloidal particles is accompanied by their separation according to the particle size; this allows one to obtain well-ordered samples of synthetic opals even if the microparticles have a broad size distribution. Phase separation of suspensions in gravitational field can also be used for preliminary separation of colloidal particles to improve their size distribution and the quality of deposited crystals.[72] Note that an ordered structure can be obtained if only the relative standard deviation of the microsphere diameters from the average value is at most 5%.[73]

Sedimentation is a very slow process which usually takes a few weeks or even months, especially, if microparticles are at most 300 nm in diameter. It can be considerably accelerated by centrifugation of suspensions; however, colloidal crystals thus obtained are characterized by poorer ordering because at high precipitation rate, the particles have no time to be separated according to their sizes. Also, the quality of colloidal crystals is strongly affected by the centrifugation rate.[74] For instance, a study of precipitation of SiO_2 microparticles 375–480 nm in diameter showed that the best results (the most ordered colloidal crystals) were obtained at a centrifugation rate of 4000 rpm; the samples obtained at centrifugation rates of 3000 and 5000 rpm were much less ordered.

The sedimentation technique faces some difficulties.[75] If the average size of SiO_2 microspheres is at most 300 nm, almost no sedimentation occurs because the energy of Brownian motion of the microspheres becomes comparable with their energy in gravitational field. Large SiO_2 microspheres (more than 550 nm in diameter) precipitate too rapidly and therefore do not form ordered structures. To accelerate sedimentation of small particles and to decrease the sedimentation rate of large particles, electrophoresis was used.[75] Since SiO_2 microspheres in aqueous suspension are negatively charged (their surface is covered with hydroxyl groups), an electric field applied to the suspension 'increased' or 'decreased' the gravitational force acting on the particles depending on the direction in which it was applied. Sedimentation of SiO_2 microspheres 870 nm in diameter led to formation of a colloidal crystal with a completely disordered structure. In turn, the use of electrophoresis allowed one to reduce the deposition rate of the particles and thus to obtain a well-ordered material. Precipitation of SiO_2 microspheres 205 nm in diameter was accompanied by electrophoresis which, on the contrary, was used to increase the precipitation rate (from 0.09 mm h^{-1} for sedimentation to 0.35 mm h^{-1}).

Yet another method of ordering colloidal particles is deposition on membranes. For instance, polymeric colloidal crystals were obtained by filtering a suspension containing latex microspheres through a polymeric membrane with nearly 100-nm pores which trapped the microspheres but let the solvent to go through.[76, 77]

Recently, the so-called vertical deposition method has been most widely used. It includes ordering of colloidal spheres on a vertical substrate under the action of capillary forces.[78–82] As a result, 'crystallization' of submicrometer-size particles at the meniscus separating the substrate and colloidal suspension upon evaporation of the solvent leads to formation of a film of the colloidal crystal with high-quality structure and allows one to rapidly obtain highly ordered, uniformly oriented colloidal crystals with controlled thickness.[78] Numerous attempts to improve the method were reported. For instance, it was shown[83] that the use of a temperature gradient provides successful vertical deposition of heavy, large SiO_2 microspheres more than 400 nm in diameter. The method of isothermal evaporation with controlled convective flows[84] allows one to obtain high-quality samples. The method of vertical deposition in an external electric field proved itself in the growth of opal films on conducting substrates.[85] Many research groups studied the dependence of the quality of the structure on the experimental conditions, *viz*., temperature,[86, 87] humidity,[87, 88] concentration of colloidal solution,[88, 89] tilt angle of the dipped substrate during the growth,[90] the nature of solvent,[91] the pH value and ionic strength,[92] *etc*. However, the results obtained in many cases cast some doubt[86] and are contradictory.[87, 88]

A fast and simple method of obtaining colloidal crystals involves ordering of polystyrene microspheres on the water surface only on heating of the suspension to 90 °C.[93] Experiments were carried out with microspheres 240 nm in diameter that formed an aqueous suspension stable over a period of a few months. However, heating causes evaporation of the solvent and the speed of Brownian motion of the microspheres considerably increases. Consequently, the concentration of microspheres in the near-surface layer of the suspension increases. The formation of ordered films of

microspheres on the surface of the solvent is favoured by a small density difference between polystyrene (1.04 g cm^{-3}) and water (1 g cm^{-3}). Further experiments revealed no formation of ordered structures on the surface of the suspension on heating if methanol having a much lower density (0.79 g cm^{-3}) was used as solvent instead of water.

In spin-coating technique a few drops of a suspension of polystyrene microspheres were placed at the centre of a substrate rapidly rotating in the horizontal plane.[94] Under the action of centrifugal force the suspension uniformly spread over the substrate surface. The process was conducted until the formation of suspension with the desired thickness. By varying the concentration of microspheres and the rotation rate one can control the thickness of the crystals.

An interesting method of ordering microspheres between two parallel plates separated by a distance of the order of a few micrometers was proposed.[95–97] The gap between the plates was sealed from three sides. The fourth side was patterned using small openings whose diameter was somewhat smaller than that of colloidal microspheres to be used. A suspension of microspheres was injected between the plates; the microspheres moved with a continuous flow of nitrogen. The openings let the fluid to go through but trapped the microspheres. The method allows one to fabricate highly ordered microsphere arrays but is of limited use because of the complexity of practical implementation and limited thickness of the final samples.

Mention may also be made of lifting of the substrate from suspension of microspheres, the Langmuir–Blodgett method, deposition of microspheres on a textured substrate and some other reviewed methods.[2–5] Yet another quite promising technique involves ordering of colloidal microparticles in a solution of photosensitive resin.[98–101] In this case, the direction of crystallization is also controlled using a narrow gap that creates geometric limitations between the substrates. Subsequent polymerization of the photoresist after exposure allows one to obtain hard photonic crystalline materials. Their distinctive feature consists in a nonclose packing of microspheres. Owing to high quality and low optical contrast the structures obtained by this method can have rather narrow stop bands and be used for engineering low-threshold lasers [100] and photonic crystalline devices that act as spectrometers.[101] In this case, microspheres are ordered simultaneously in the bulk rather than in layer-by-layer fashion; therefore, the formation of structural defects should proceed in different manner compared to other methods.

2. Template methods of synthesis of inverse opals

Colloidal crystals are often used as templates for the synthesis of inverse structures from various materials.[73, 102] This approach is attractive owing to its versatility because it allows one to synthesize photonic crystals based on metals,[32, 77, 103–114] nonmetals,[83, 115–119] oxides,[25, 42, 62, 74, 76, 105, 120–149] semiconductors,[12, 119, 150–157] polymers,[95, 127, 158–161] *etc*. Although each synthesis has its specific features, there are some common stages characteristic of template synthesis that depend on the chemical nature of the final product (Fig. 4).[73]

The first stage involves the synthesis of a colloidal crystal. Next, this crystal acts as a template which is wetted with a fluid that is transformed to a hard cage under the action of various physicochemical factors. Voids in the

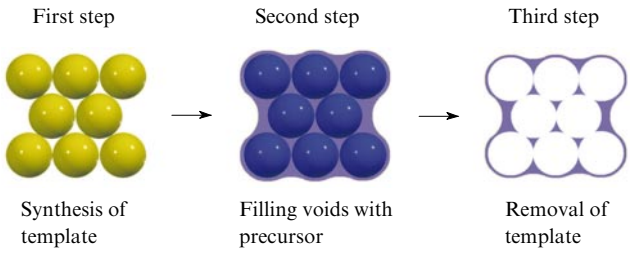


Figure 4. Template synthesis of inverse opals: a scheme.

template structure are filled using chemical vapour deposition (CVD), electrochemical deposition, introduction of melt, *etc*. Specific features of chemical reactions in pores of opal templates have been documented.[162, 163] Finally, colloidal template spheres are removed by dissolution or thermal decomposition (in the case of polymeric microspheres). The structures thus obtained are often called inverse opals. Clearly, the microspheres used to form the template should be wetted by precursors and readily removed under conditions in which the inverse structure retains its stability.[73]

Considerable attention is paid to the synthesis of inverse opals from high-index compounds. For instance, a structure comprised of thin hollow silica spheres with a complete photonic band gap at about 1.46 μm (see Fig. 1) was successfully obtained using an opal template and the CVD method.[12] Among compounds transparent in the visible region, rutile (TiO_2) seems to be attractive. The compound has an anisotropic refractive index higher than a value of 2.9 for one direction of polarization. In principle, this is sufficient to open a complete or almost complete photonic band gap in the inverse opal.

Inverse opals based on titania were for the first time synthesized independently by researchers from the Netherlands [120] and the USA [121] using polystyrene colloidal crystals as templates; structural voids were filled with a titanium alkoxide [*e.g.*, $Ti(OEt)_4$]. Owing to high reactivity of $Ti(OEt)_4$ (hydrolysis resulting in hydrated amorphous titania takes a few minutes in air) this procedure was carried out in a dry box in inert (nitrogen or argon) atmosphere. Once the sample was removed from the box, titania in the template voids was formed as a result of the reaction of titanium alkoxide with atmospheric moisture. Wetting of the colloidal crystal with the liquid precursor and subsequent hydrolysis can be repeated numerously until complete filling of the template voids with titania. In the last stage, colloidal microspheres were removed from the structure by thermal decomposition or dissolution in the corresponding solvent (*e.g.*, toluene).

It should be noted that researchers from the USA [121] positioned porous titania they have synthesized as a promising material for catalysis, sorption and separation of organic substances, while the aim of researchers from the Netherlands [120] was to synthesize a material with unique photonic properties. A study [120] of the reflection of an inverse opal based on TiO_2 along the $\langle 111 \rangle$ direction predicted the possibility of existence of a complete photonic band gap. Despite the lack of experimental proof of this assumption, inverse opals based on TiO_2 have long been considered as the most promising materials for photonics (see, *e.g.*, Refs 62, 122, 124, 128–134, 141) and Ref. 120 has

been among the most widely cited publications in this field. More recently, colloidal crystals from not only polymeric, but also silica microspheres were used as templates. In the latter case, the template material is removed by dissolution of amorphous SiO_2 in concentrated aqueous alkali on heating.[131, 132]

In spite of apparent simplicity of the method and uniqueness of the optical properties of rutile, obtaining a macroscopic inverse opal suitable for characterization of its physical properties faces severe difficulties. This is to a great extent due to the fact that annealing is accompanied by dehydration and sintering of amorphous titania; as a result, the lattice constant of the inverse opal decreases while the samples undergo intense cracking.[120, 121, 128] Moreover, the early stage of annealing of amorphous titania is accompanied by crystallization of anatase having a lower refractive index while subsequent recrystallization to rutile also leads to breakdown of the ordered structure of the inverse opal.

A year after publication of the first studies on the synthesis of photonic crystals based on TiO_2 a new method was proposed, which allows one to obtain rather large samples (to 1 cm in size). The method uses presynthesized nanoparticles of the desired TiO_2 polymorph rather than the liquid precursor of titania. Different versions of the method involve multiple wetting of the colloidal crystal with a suspension of nanoparticles[131] or co-deposition of colloidal microspheres and TiO_2 nanoparticles (during self-organization of large microspheres into a 3-D matrix, nanoparticles occupy its voids) with subsequent removal of microspheres.[123, 124] The advantage of this approach consists in minimization of undesired cracking of photonic crystals on heat treatment, which significantly improves the quality of samples.

It should be noted that even the authors of the most successful studies on the synthesis of inverse TiO_2 opals including the authors of recent publications[146, 147] did not observe a complete photonic band gap, in particular, because of insufficient quality of samples. Therefore, main efforts of researchers were aimed at obtaining photonic crystals based on materials that exhibited certain useful functional properties rather than high-index materials.

A number of studies were devoted to the synthesis of inverse opals based on $A^{II}B^{VI}$ semiconductors. In particular, CdS and CdSe are characterized by rather high refractive indices (2.5 at 600 nm and 2.75 at 750 nm, respectively), being optically transparent in the visible and near-IR regions, and have valuable luminescent properties. In particular, SiO_2 synthetic opals were dipped into a suspension of CdSe quantum dots in decane.[152] Since the size of the cross-section of the narrowest channels in the opal structure is two orders of magnitude larger than the sizes of semiconductor nanoparticles, the latter penetrated with ease into all structural voids of the template. Subsequent evaporation of the solvent and etching of SiO_2 with dilute hydrofluoric acid led to formation of inverse opals based on CdSe. Attempts to synthesize porous media based on the semiconductors CdS and InP were also undertaken in the early studies (see, *e.g.*, Refs 1, 164 and 165); however, voids in the template structure were filled only partially.[152]

Yet another approach to the inverse opals based on $A^{II}B^{VI}$ semiconductors is electrochemical deposition. It was used to obtain photonic crystals based on the semiconductors CdS and CdSe with polystyrene colloidal crystals as templates.[151]

Semiconductors $A^{III}B^{V}$ (*e.g.*, GaP, GaN and solid solutions based on them) are also rather promising materials for the synthesis of inverse photonic crystals.[155, 156] These semiconductors are transparent in the visible region and have high refractive indices. In addition, they exhibit luminescent properties which are widely used in modern semiconductor optoelectronics. Inverse opals based on GaP, GaN and GaP_xN_{1-x} are promising for investigations of the effect of photonic band gap on spontaneous emission of light. The semiconductors GaP, GaN and GaP_xN_{1-x} can be synthesized directly in pores of the SiO_2 opals. Initially, pores are filled with gallium oxide (Ga_2O_3) using aqueous solutions of gallium salts as precursors. Next, the samples are annealed in ammonia or phosphorus hydride atmosphere. The template matrix is removed by etching silica spheres with a 10% solution of hydrofluoric acid.

Of particular interest are metallic inverse opals which, on the one hand, have high conductivity and, on the other hand, exhibit unusual optical properties due to the specific photonic band structure of metallic photonic crystals.[166–169] Using such metals as Fe, Ni, Co, one can obtain magnetic inverse opals promising for magnetooptics. Clearly, electrochemical deposition is the simplest method for filling structural voids in the colloidal crystal with metals. In particular, it was used to obtain inverse opals based on Ni, Au, Pt, Pd and Co.[109, 110, 113, 114] Note that electrochemical deposition is also suitable for obtaining inverse opals based on some nonmetallic compounds (V_2O_5,[145] CdS, CdSe,[151, 170] ZnO[171, 172]). At the same time, in the synthesis of metallic photonic crystals internal voids of the colloidal crystal can be filled with metallic nanoparticles similarly to the synthesis of inverse opals based on TiO_2 and CdSe. This method was used to synthesize[111] inverse opals based on gold using gold colloidal nanoparticles 15–25 nm in size.

Inverse opals based on electrochromic materials, in particular, the oxides WO_3, V_2O_5 and VO_2, can controllably change their colours and refractive indices depending on the applied voltage. Therefore, they are promising for fabrication of optical switches. It should be noted that WO_3 has cathodic electrochromism, VO_2 exhibits anodic electrochromism while V_2O_5 demonstrates either cathodic or anodic electrochromism depending on the spectral region.

A method for synthesis of inverse opals based on WO_3 is as follows.[135, 136] First, the template matrices are synthesized. These are colloidal crystals based on monodisperse submicrometer-size polystyrene spheres. Next, a tungsten oxide precursor is prepared. To this end, metallic tungsten is dissolved in a mixture of 30% hydrogen peroxide and acetic acid and the solution is filtered and evaporated to dryness. The reaction of the powder thus obtained with ethanol results in a WO_3-based sol which is used to fill pores in the template matrix. In the final step, the template is repeatedly dipped in this solution (the tungsten oxide sol is rapidly aged in air) and then the sample is annealed at 460 °C for 1 h to remove the polystyrene template.

Inverse opals based on vanadium oxides are also synthesized by the template method using, *e.g.*, synthetic opals based on monodisperse silica spheres as templates.[137, 138] Pores in the opal matrices were filled with a vanadyl nitrate solution and then the oxide V_2O_5 obtained by thermal decomposition was reduced to VO_2 by high-temperature annealing in vacuum. The SiO_2 template was removed by dissolution in hydrofluoric acid. More recently, an inverse

opal was also synthesized from V_2O_5 using electrochemical deposition.[145]

Noteworthy is a study[115] on the synthesis of inverse opals based on carbon. Voids in the structure of the synthetic opal were filled with carbon and the SiO_2 microspheres were removed by dissolution in hydrofluoric acid. Structural voids in the opal were filled using two methods, (i) CVD and (ii) impregnation with phenol–formaldehyde resin followed by pyrolysis at 1000 °C. In some cases, diamond nanoparticles 2–5 nm in size were introduced into the structure of the synthetic opal; they acted as seeds for the growth of diamonds. Treatment of the composite with methane–hydrogen plasma and subsequent removal of the SiO_2 microspheres by dissolution in HF led to inverse opals based on diamond.

The authors of study[115] seem to be the first who pointed that inverse opals themselves can act as templates for the synthesis of opal-type photonic crystals based on metals, semiconductors and superconductors. In this case, one can obtain materials with unique combinations of optical, electrical and magnetic properties. Inverse opals were used as templates in more recent studies.[105, 127] In particular, approaches using silica and polymers as templates were combined.[127] First, a synthetic opal based on SiO_2 microspheres was impregnated with a liquid monomer. As structural voids in the template were filled, the monomer polymerized as a result of chemical and photochemical reactions. Subsequent dissolution of SiO_2 in dilute hydrofluoric acid led to the formation of a polymeric inverse opal. Then, voids in the polymer structure were filled with various substances using methods analogous to those described above.[120, 121] The final stage involved thermal decomposition of the polymer which resulted in opal-type photonic crystals based on metals (Au and Ni) and various inorganic compounds (TiO_2, ZrO_2, Al_2O_3, CdS and AgCl).

Opal-type photonic crystals based on gold were synthesized in a somewhat different manner.[105] In the first step, a synthetic opal based on SiO_2 microspheres was placed on a gold substrate and then voids in the template structure were filled with metallic nickel by the electrochemical method. Then, SiO_2 microspheres were dissolved in 2% solution of hydrofluoric acid. In the second step, the nickel inverse opal was annealed at 550 °C in air. As a result, nickel was oxidized to NiO. Finally, voids in the porous structure based on nickel oxide were filled with metallic gold using electrochemical method and subsequently NiO was dissolved in boiling dilute sulfuric acid.

As mentioned above, a key advantage of the template method is its versatility. The approach is common to many classes of compounds and can be used to obtain porous structures based on SiO_2, Sb_4O_6, WO_3, $ZrO_2(Y_2O_3)$, NiO, Co_3O_4, Mn_2O_3, MgO, $CaCO_3$, ZnO, Fe_2O_3 and Cr_2O_3.[122, 125] In some cases, alkoxides as precursors of metal oxides were replaced by the corresponding oxalates which decomposed *in vacuo* in the temperature range 240–420 °C. In this situation, the following products can be formed depending on the ionic radius of the metal and its oxygen affinity:

a metal carbonate

$$MC_2O_4 \longrightarrow MCO_3 + CO\uparrow,$$

where M = Ca, Sr or Ba;

a metal oxide

$$MC_2O_4 \longrightarrow MO + CO_2\uparrow + CO\uparrow,$$

where M = Mg, Mn, Zn, Fe or Sn; or

a metal

$$MC_2O_4 \longrightarrow M + 2CO_2\uparrow,$$

where M = Co, Ni, Cu or Pb.

Note that the products of the last two reactions can undergo oxidation in air in the specified temperature interval.[122, 125]

In this Section, some (but by no means all) of compounds suitable for the synthesis of inverse opals are considered. Figure 5 presents the electron micrographs of some inverse opals described in Ref. 144. However, despite the variety of the inverse structures obtained by the template methods, they have some common features. In all cases, one deals with inversion of the template matrix; therefore, the inverse opal inherits many properties from the initial colloidal crystal. In particular, the optical properties of an inverse opal are determined by the lattice constant and by the crystallographic orientation of the template matrix. Real colloidal crystals and inverse opals also have many common structural features. It is structural imperfection of the template matrix that to a great extent determines the defectiveness of inverse opals, although the inversion procedure (filling of voids in colloidal crystal, heat treatment) leads to additional violation of the structural periodicity.

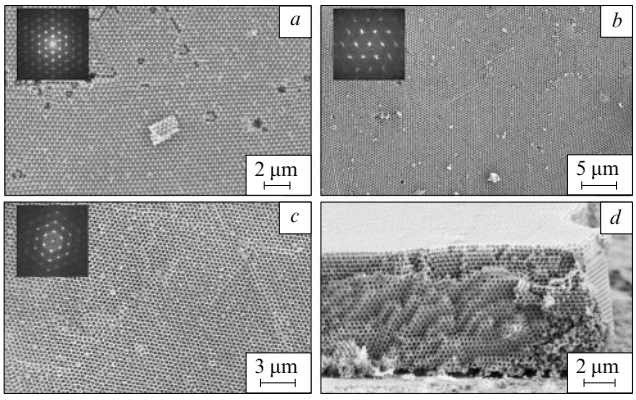


Figure 5. Electron micrographs of inverse opals based on Fe_2O_3 (*a*), TiO_2 (*b*), SiO_2 (*c*) and TiO_2 (cleavage) (*d*).[144]
Insets: the Fourier transforms of the micrographs.

IV. Structural features of opals and inverse opals †

In the synthesis of opals, colloidal microspheres are self-organized into close-packed stackings[78, 173] composed of closest-packed hexagonal layers of spheres. Each layer can occupy one of three possible spatial positions, namely, *A*, *B*

† The real structure of synthetic opals and inverse opals will mainly be described taking samples obtained by the most widely used methods (sedimentation and vertical deposition) and the inverse structures based on them as examples.

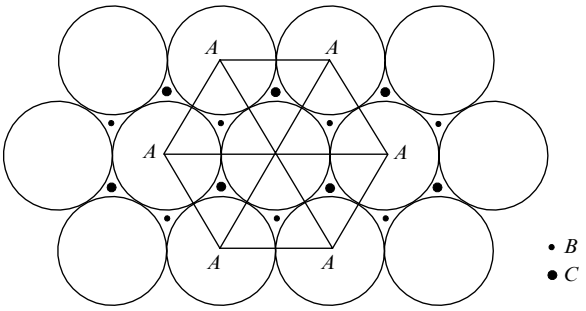


Figure 6. Relative arrangement of close-packed layers of beads: positions *A*, *B* and *C*.

(shifted from position *A* by $\boldsymbol{a}_1/3 + 2\boldsymbol{a}_2/3$) or *C* (shifted from position *A* by $2\boldsymbol{a}_1/3 + \boldsymbol{a}_2/3$), where $\boldsymbol{a}_1$ and $\boldsymbol{a}_2$ are the translation vectors of the hexagonal lattice in the layer (Fig. 6). The *ABABAB* stacking gives a hexagonal closest packing (hcp), whereas the *ABCABC* or *ACBACB* stacking corresponds to a fcc structure. The only necessary condition for the closest packing is that the neighbouring layers *N* and $N+1$ be shifted relative to each other (have different spatial positions). Thus, a crystal based on microspheres can consist of arbitrarily alternating close-packed layers. If α is the probability for the layers *N* and $N+2$ to occupy different positions, the case $\alpha = 1$ will correspond to the fcc structure, $\alpha = 0$ corresponds to the hcp structure, and $\alpha = 1/2$ corresponds to the random hexagonal close packing (rhcp) with random alternation of hexagonal layers in stacks.

It is believed that the main reason for ordering of spherical microparticles in the self-assembly of a colloidal crystal is an increase in the entropy of the system.[174, 175] Clearly, the configurational entropy decreases on ordering; however, an increase in the entropy related to the free volume per particle is more significant. The model of solid noninteracting microspheres predicts that ordering into the fcc structure leads to a somewhat higher free energy gain compared to the ordering into the hcp structure.[176] The difference between them is rather small; therefore, synthetic opals contain not only the fcc-like structural fragments,[177] but also stacking faults due to violated stacking sequence.[178] Synthetic opals also contain many other types of defects known for atomic crystals, such as small-angle interblock boundaries, linear defects (*e.g.*, dislocations) and various point defects (vacancies, bivacancies, interstitials; some of them occur with a probability of 1 defect per 50 – 100 unit cells).[72, 178]

These defects are typical of most opals and inverse opals. However, there are also structural features characteristic of particular methods of synthesis. For instance, considering sedimentation, the sample is usually divided into a variety of misoriented microscopic domains separated by disordered regions.[72, 179] This is due to the fact that in the deposition of colloidal particles, each domain grows from its own seed independently. Clearly, research and practical use of such opals requires selection of monodomain regions, which is sometimes difficult.

At the same time, films of colloidal crystals obtained by the method of vertical deposition under appropriate conditions are characterized by much higher quality of the structure compared to sedimentation opals.[83] As a rule, they

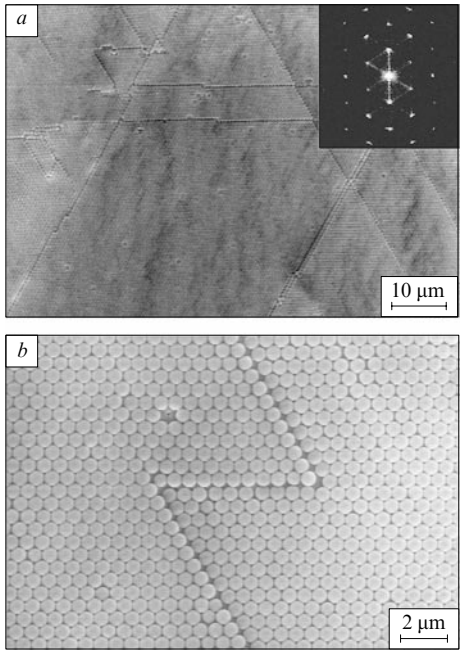


Figure 7. Electron micrographs of the surface of opal-like film grown from polystyrene microspheres 655 nm in diameter.[180]
(*a*) Inset: Fourier transform of the micrograph indicating a highly ordered structure;
(*b*) clearly seen structural defects characteristic of the opal film, namely, vacancies and extended defects in the form of zigzag lines on the surface; the latter can be due to tilted double stacking faults.[181]

have hexagonally packed layers parallel to the substrate surface (Fig. 7). Although the films consist of domains separated by cracks, all domains have the same orientation[82, 182, 183] and there are almost no disordered regions. Most probably, separation into domains occurs after deposition due to shrinkage on drying. Also, domains whose size can reach a value of 1 mm hold their initial orientation related to the direction of the motion of the meniscus.[89] The advantage of this method is that colloidal crystals are much more prone to form regular fcc structures. The reason for this is still unclear. As mentioned above, in the model of solid noninteracting microspheres, the free energy difference between the fcc and hcp structures is so small that determination of the energy minimum requires long-term crystallization.[173] In the case of vertical deposition, the crystallization front moves rapidly; therefore, the reason for preferred formation of the fcc structure is probably related to the kinetic features of the process. In this connection, it was assumed[184] that the formation of the fcc packing is due to some features of passage of the solvent flow through the growing structure. However, this was not confirmed experimentally.[185]

Observations[185] as well as model experiments showed that the first three layers in the crystallization front mainly have the *ABA* rather than *ABC* stacking sequence, as should be in the growth of the fcc structure. However, the probability of the fcc ordering increases with the distance from the substrate. Interestingly, seeding each new layer is accompanied by the appearance of a narrow area with the symmetry of a square parallel to the growth front on the film surface. It is believed that the regions with a transient

structure forming in the seeding of each new layer are of fundamental importance for the mechanism of formation of the fcc packing of films. The results of modeling of a transition from the two- to three-layer structure also confirmed the formation of a square region in the transition region.[185] At the same time, if the film can be considered thick, the reason for the formation of a square transient region upon addition of one more new layer is still to be clarified. It was assumed [186] that the new layer is formed at the interface with the substrate rather than on the film surface and the existing layers are seemingly stretched on the terrace thus formed. Probably, the formation of the square structure is due to the accompanying deformations.

In spite of relatively high quality of films obtained by the method of vertical deposition, they often contain stacking faults. Regions with different stacking sequences (so-called twins) are often spatially separated. This is the reason for the appearance of a characteristic strips.[187] Dark and light strips are observed in the transmission geometry (detection normal to the surface) at nonzero angle of incidence. As the angle of incidence changes its sign, the dark and light strips interchange. At normal incidence, a uniform pattern is observed. The appearance of strips is due to the fact that they correspond to twins in the fcc structure with different stacking sequences (*ABC* and *ACB*).

As mentioned above, inverse opals inherit defects from the initial template. In addition, additional more or less pronounced cracking and separation into domains occur in inverse opals depending on the method of inversion, degree of filling of voids in the template and the sintering temperature.[188] In turn, the domain structure can also undergo deformations, be misoriented relative to the template and contain a large number of additional defects (vacancy complexes and microcracks). Since the higher the solubility of the precursor salt the higher the degree of filling of voids in the template, the quality of the structure of inverse opals correlates with the solubility of the precursor salts. For instance, if the precursor is a solution of zinc nitrate in aqueous ethanol, one can obtain good-quality inverse ZnO films with a low degree of cracking.[143] The solubility of zinc nitrate is two times higher than that of aluminium nitrate; consequently, inverse Al_2O_3 films obtained using aluminium nitrate have a small-size island structure. These structural defects do not appear in the case of electrochemical deposition. Inverse metallic films obtained by electrochemical deposition are at least competitive in quality with the corresponding templates. The advantages of this method also include the possibility to control the film thickness by measuring the electric charge transferred in the course of deposition.[189]

Many researchers noted that structural imperfection of colloidal crystals has a negative effect on their photonic band structure and optical properties,[5, 186] being the main difficulty for practical use. In particular, the band structure is strongly influenced by the stacking faults.[178, 190] Meanwhile, the spectral position of the first photonic stop band at the *L* point of the Brillouin zone is independent of the stacking sequence and therefore it is relatively insensitive to this type of defects. The behaviour of the stop bands along the ΓL direction was modeled [190] and small differences between their patterns for all close-packed structures were reported. At the same time, stacking faults lead to uncontrolled appearance of allowed modes in the higher-order stop bands.

The size dispersion of colloidal particles may have even more pronounced effect. It was established that an increase in the particle size dispersion leads to increase in the number of all types of point and linear defects.[191] But what is most important, due to size dispersion all microspheres, even in the structurally perfect regions, are shifted from ideal crystallographic positions, thus producing light scattering. This seems to be the main reason for small free path length of photons in the opal structures (about 15 μm),[192] which influences all properties of opals and inverse opals related to their photonic band spectrum. This problem was investigated experimentally.[193, 194] Changes in the structural and optical properties of opal films on doping with microspheres of 'incorrect' size were studied. An increase in the concentration of 'alien' microspheres led to violation of long-range order and significant deterioration of the optical properties related to the first photonic stop band. This problem was also touched in the studies [42, 43] on the radiation patterns of the opal and inverse opal thin films containing luminescent complexes. According to calculations of the spatial distribution of the density of optical states, the intensity of radiation emitted from the samples with perfect structures should abruptly change depending on the direction, namely, be suppressed along the directions of the stop bands and enhanced along the directions with high density of optical states. However, the radiation patterns appeared to be highly smoothed. It is believed [43] that the differences between the results of calculations and experimental data are due to the diameter dispersion of spheres. Because of this, different emission centres are in different local environment and have different radiation patterns which are then averaged over the ensemble of such centres.

One more aspect of investigations of the structure of opals based on SiO_2 microspheres is related to its fractality:[195–197] large SiO_2 microspheres about 1000 nm in diameter are comprised of the second-order globules about 100 nm in diameter, which in turn are composed of smaller (third-order) nanoglobules. The spheres have relatively loose cores and hard shells formed on sintering.[198, 199] These features affect the properties of opals as photonic crystals. In particular, in a model medium with homogeneous spherical microspheres, the periodic structure and the Bragg diffraction will disappear if voids are filled with a liquid having the same refractive index as that of the microspheres. However, in a real opal with inhomogeneous microparticles the Bragg diffraction can in principle not disappear simultaneously along all directions. Different stop bands disappear in opals at different refractive index of the filler.[198–201] By varying this coefficient one can selectively 'switch off' particular stop bands. Note that in sintering of opals, neighbouring microparticles become linked and their shapes thus differ from spherical shape. This should sometimes be taken into account in calculations of the photonic band spectrum.

V. Methods of investigation of structural defects in opals and inverse opals

1. Microscopy and optical spectroscopy

The results of scanning electron microscopy (SEM) and atomic force microscopy (AFM) studies only allow one to assess the ordering of the top layer of microspheres in the case of colloidal crystal and a few layers of air voids in the

case of an inverse opal. A SEM study [78] established that the dense top layer of microspheres in colloidal crystal films obtained by the vertical deposition method is ordered on the length scale of a few millimeters and that domains in the opal structure are characterized by small misorientation. However, we do not know what is the stacking sequence in the interior of the films. The study of the cleavage of a crystal is often difficult owing to breakdown of the structure; in addition, there is no warranty that the stacking pattern observed at the cleavage extends to the entire crystal (or its large part). Electron microscopy studies are additionally complicated by the need to coat non-conducting samples (most samples indeed) with a conducting layer, which makes them inappropriate for the optical experiments. In addition, the structure of the sample can be influenced by the micrography conditions.

Yet another method of investigation of the structure of colloidal crystals is confocal microscopy.[202, 203] It requires a specific sample preparation procedure, *viz*., scattering should be minimized by decreasing the refractive index to the maximum possible extent and luminescent labels should be introduced to obtain the image. By successively focussing the microscope on different layers and comparing the images one can obtain information on sample structure.

Defects first of all affect the optical properties; therefore, it seems logical to use the optical properties for the determination of the quality of the structure. The defectiveness of a sample can be characterized by modeling diffusion scattering through absorption, *i.e*., by treating the effective refractive index as a complex parameter whose imaginary part increases with the number of defects in the sample.[204–206] Clearly, this approach gives only a qualitative idea of the defectiveness and provides no knowledge of which defects play the role of scattering centres.

The optical properties of a sample are best characterized by the transmission and reflectance spectra obtained for different crystallographic directions. The energy band structure of sedimentation opals along the L_g-K_g-L-P, L_g-W_g-K and $P-K$ directions of the Brillouin zone was measured experimentally.[207] The subscript 'g' denotes that the specified point of the Brillouin zone belongs to the face that is parallel to the close-packed (111) growth planes. By and large, the results of measurements confirmed a twin fcc structure of the opal. In particular, it was found that minimum in the transmission spectrum corresponds to the L point of the Brillouin zone is weaker and broader than the minimum corresponding to the L_g point; this can be explained by a larger number of stacking faults along the directions differing from the growth axis.

Recently, quick methods of structure determination of colloidal crystals based on analysis of their optical images have been developed. Optical micrographs allow one to visually distinguish between the ABA and ABC three-layer stacks. Namely, if the particle size is rather large, high-order bands appear in the visible region (the behaviour of these bands is influenced by the stacking pattern to the greatest extent).[208–210] For this reason, the absorption by the ABA and ABC stacks is different and they differ in colour. A similar analysis can also be performed for the four- and five-layer samples; however, analysis is strongly complicated with an increase in the number of layers (N) because the number of possible closest stacks increases as 2^{N-2}. In addition, under particular photomicrography conditions (at very narrow aperture), one can distinguish between differently coloured point defects, grain boundaries and dislocations in the optical micrographs.

2. Features of diffraction from opal type structures

A reflection appears if the Ewald sphere in the reciprocal space simultaneously passes through two nodes of the reciprocal lattice.[211] By analyzing the diffraction patterns at different positions of the Ewald sphere (*i.e*., at different angles of light propagation in the crystal) one can construct a reciprocal lattice of the sample under study and then reconstruct the structure in the direct space. Diffraction experiments involve measurements of the intensity of radiation, which in the simplest case of structures composed of the same particles is equal to the product of the structural factor (characterizing the reciprocal lattice) by the form factor (characterizing the unit scattering element).[211] The structural factors of the fcc and hcp lattices are well known. In particular, for the fcc packing, all allowed diffraction reflections are characterized by the same structural factor and the diffraction intensity is determined by the form factor (F) which can cause some reflections to weaken considerably. In the small optical contrast approximation, the form factor of a uniform spherical particle is given by [212]

$$F = \frac{9[\sin(kR) - kR\cos(kR)]^2}{(kR)^6},$$

where k is the wave number and R is the radius of the sphere. This relation works well in the case of X-ray diffraction. For diffraction of visible light, there may be the need for more complex calculations using the Mie theory [213] which takes into account the real value of the refractive index of the material of the scattering sphere.

In the case of defect structures, the description of the reciprocal space is more complicated. The theory of diffraction from structures with stacking faults was initially developed for conventional crystals (Wilson's theory).[212, 214] Model calculations of the structural factor at different values of the parameter α (stacking probability, see Section IV) were also reported for colloidal crystals.[215] If the structure represents an array of identical layers stacked in some way, the structural factor of this system can be represented by the product of the structural factor of an individual layer and a factor which contains information on the stacking sequence.

The reciprocal lattice of an individual close-packed layer of spherical microparticles represents a hexagonal system of (hk) rods separated by a distance of $4\pi/(3^{1/2}a)$, where a is the diameter of the sphere. The sites of the reciprocal lattices of the fcc and hcp structures also lie on these rods. If the Miller index difference ($h-k$) is not a multiple of three, the structural factor of any defect packing differs from zero at all points of the rod. Extended objects appearing in this case in the reciprocal space are known as Bragg rods.[215, 216] If the difference ($h-k$) is a multiple of three, the structural factor is independent of the stacking sequence. For any α value, the structural factor along these rods represents a set of δ-peaks (so-called Bragg points).[215]

3. Microradian X-ray diffraction

As mentioned above, microscopy studies of the structure in the bulk of samples face severe difficulties. For instance, what are thin extended defects that appear as lines on the surface of colloidal crystal film (see Fig. 7)? Are these

interblock boundaries, dislocations, tilted stacking faults, or something else? What is the preferred structure in the sample, namely, fcc, hcp or rhcp? Answers to these questions may be obtained by diffraction methods of investigation, which allow one to obtain comprehensive information on the structure of the object under study. Among them, the method of microradian X-ray diffraction seems to be the most informative. This is an indispensable method of investigation of the structures with small lattice constants, which cannot be studied by diffraction of visible light.

Diffraction of X-ray and neutron radiations from colloidal crystals has some features. First, the wavelength of incident radiation is much smaller than the characteristic lattice constant; therefore, usually one deals with very small-angle scattering, and the Ewald sphere has a negligible curvature. In calculations, the Ewald sphere is usually taken to be flat. Second, for a given range of wavelengths the refractive index of any medium with a rather high accuracy has the same value equal to unity. The lack of refraction also significantly simplifies calculations.

The first experimental neutron diffraction studies [217–221] on the structure of colloidal crystals were not very informative due to the low beam intensity and monochromaticity. Nevertheless, a comparison of the diffraction patterns obtained at different angles of incidence of radiation suggested the rhcp structure of the sample.[221]

Diffraction of synchrotron radiation was for the first time implemented using colloidal single crystals [222] and then on inverse opals.[134] The observed diffraction sequence was indexed for the fcc structure and it was emphasized [134] that all reflections corresponded solely to the fcc stacking pattern, *i.e.*, the region under study was free from twins and stacking faults. Since then, a variety of experiments using synchrotron radiation were carried out.[216, 223–228] The existence of Bragg rods in a colloidal crystal with rhcp structure was for the first time established based on experimental data [216] and a change in the character of the diffraction patterns on drying of a colloidal crystal as well as the loss of long-range order was demonstrated.[225]

Various films of inverse opals based on titania, silica and iron(III) oxide were studied by microradian X-ray diffraction.[144, 229] The samples mainly had a twin fcc structure with some contributions of the hcp and rhcp structures. The ratio of fragments with different structural types was different for different samples. As an example, Fig. 8 presents the intensities of some diffraction reflections plotted *vs.* angle of rotation of the sample around the axis lying in the surface plane. At a chosen direction of the axis of rotation of the sample, reflections corresponding to the *ABC* and *ACB* stacking sequences were mirror symmetric. Both types of reflections were observed. Based on their reflection intensity ratio, it was established that the ratio of the volume fractions of the fcc fragments with the *ABCABC*... and *ACBACB*... stacking sequences is about 2 : 3. No reflections corresponding to the hcp structure were observed for the sample. Thus, small-angle X-ray diffraction allows one to reveal a preferred type of the close-packed structure, as well as fragments with other types of stacking, and to determine the ratio of the fcc fragments with different sacking sequences (*ABCABC*... and *ACBACB*...).

Microradian X-ray diffraction studies also disclosed a new type of structural defects in colloidal crystal films, namely, double stacking faults propagating at an angle of

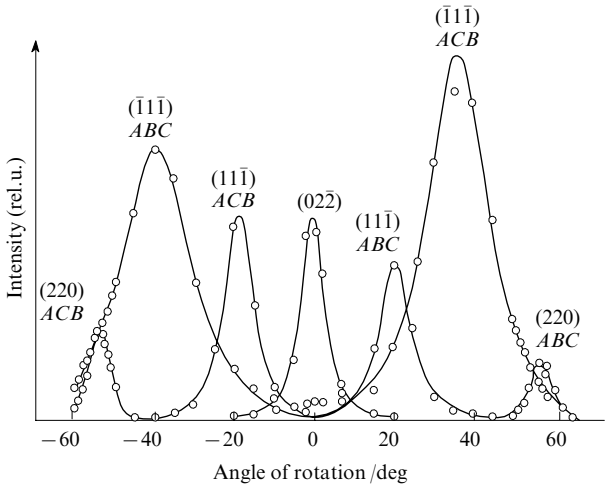


Figure 8. Intensities of different reflections plotted *vs.* angle of rotation of the sample.[229]
Open circles denote experimental data, solid lines denote approximation of the peaks by the Lorentz functions.

70.5° to the film surface.[181] Nearly 10% of all stacking faults belong to this type of defects.[181] In the direct space, they look like a characteristic terrace with the symmetry of a square and variable height relative to the top layer (see Figs 7 *b* and 9). Earlier, this type of defects was treated as a kind of linear defects.[191] Also, the structure of a small region of an opal film (0.5×0.5 mm^2 in size) in the reciprocal space was constructed using small-angle X-ray diffraction data.[230]

4. Laser diffraction

Technically, laser diffraction is much less sophisticated than diffraction of synchrotron radiation. However, obtaining information on the internal structure of photonic crystals by laser diffraction is much more complicated because one should take into account refraction and carry out complex calculations of the form factor of spherical particles using the Mie theory. An important limitation for application of diffraction of visible light is that it will be observed only for structures with a spatial period of no less than the wavelength of the light used.

Laser diffraction was used before the emergence of interest in colloidal crystals as materials for photonics in the simulation of processes in conventional crystals using colloidal microspheres (*e.g.*, crystallization, melting under shear strain [173, 231]). In a number of studies (see, *e.g.*, Refs 173, 232 and 233), the structures of colloidal crystals were determined by powder laser diffraction (analogue of powder X-ray diffraction for conventional crystals). Diffraction of visible light was used for fast determination of the degree of structural ordering from the quality of the diffraction pattern observed at normal incidence of light.[234–240] Laser diffraction is particularly convenient for the determination of the lattice constants of photonic crystals using the expression

$$nd[\sin\theta + \sin(\theta - \varphi)] = \lambda,$$

where n is the refractive index of the medium whose diffraction pattern was recorded;

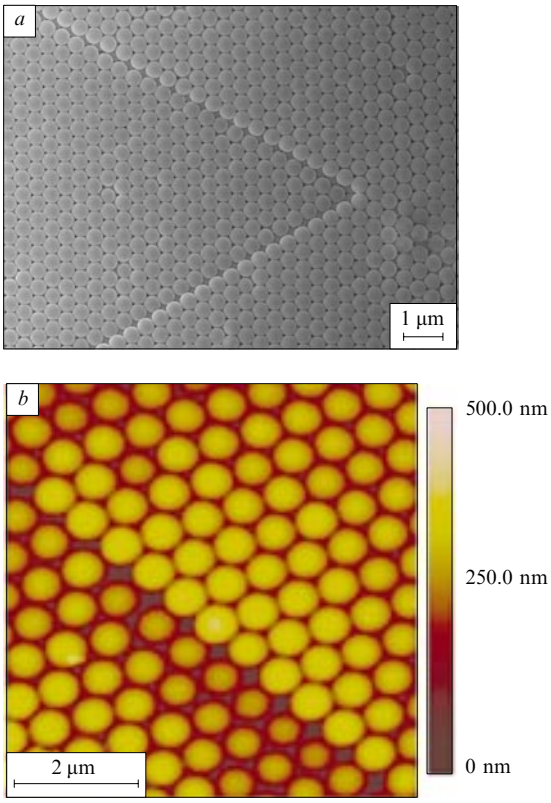


Figure 9. Manifestation of tilted double stacking faults in the top close-packed layer of an opal film according to electron microscopy (*a*) and atomic force microscopy (*b*) data.[181]

$$d = a\frac{\sqrt{3}}{2},$$

a is the effective diameter of the microsphere; θ is the angle of incidence of laser beam calculated with respect to the normal to the sample surface; φ is the angle between the diffracted and transmitted beams; and λ is the laser wavelength in vacuum.[142, 235]

A dependence of the intensity of a diffraction reflection on the angle of incidence of radiation was obtained experimentally.[235] To interpret the results obtained, numerical modeling was carried out. Analogous dependences were calculated for the fcc (with the *ABC* and *ACB* stacking sequences), hcp and rhcp structures by simply adding the scattering intensities from all spheres. Scattering from particular spheres were calculated using the Mie theory. Summation of the scattering intensities from different spheres was carried out in two steps. First, the scattering from a perfect close-packed layer was calculated and then summation over a particular number of layers of specified orientation was done. A comparison of the results of calculations with experimental data revealed a twin fcc structure. The authors also proposed and implemented a method for the synthesis of the fcc structures without twinning. To this end, crystallization was carried out under a small shear strain parallel to the close-packed planes of crystal. At small shear strain, a diffraction pattern from three points (*cf.* six points with no strain) was observed. Interestingly, unloading was followed by relaxation of the crystal and a diffraction pattern from six points was observed again, which seems to correspond to the twin fcc structure.

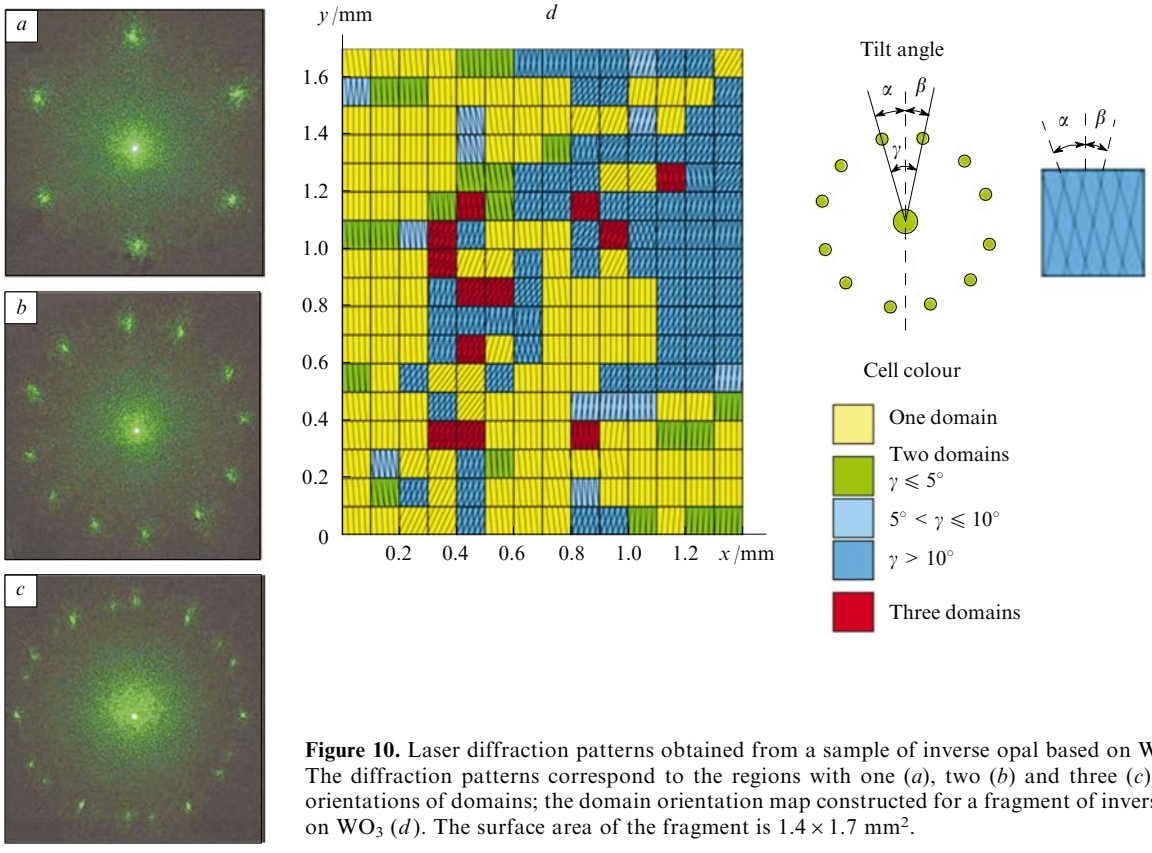


Figure 10. Laser diffraction patterns obtained from a sample of inverse opal based on WO_3.[139] The diffraction patterns correspond to the regions with one (*a*), two (*b*) and three (*c*) well-defined orientations of domains; the domain orientation map constructed for a fragment of inverse opal based on WO_3 (*d*). The surface area of the fragment is 1.4×1.7 mm^2.

A laser diffraction structural study of ordered colloidal suspensions was performed and the intensities of diffraction reflections at different angles of incidence of laser beam on the sample were determined.[241] The intensity distribution along the (10) Bragg rod was calculated from the dependence of intensity on the angle of incidence of laser beam. Depending on the ordering time of the system, different values of the stacking probability parameter α, namely, from about 0.5 to nearly 0.8 were observed. The appearance of two symmetrically arranged reflections for the incidence of laser radiation along the ΓP direction was observed.[207] These reflections were ascribed to two types of the fcc structure (with the ABC and ACB stacking sequences) and thus twinning in the structure was proved. Note that the colloidal crystals investigated in the studies [207, 235, 241] were characterized by very low contrast of the refractive indices; this facilitated calculations.

Diffraction in the region of high-index bands of the photonic spectrum of a colloidal crystal was studied.[242] The diffraction patterns observed were in qualitative agreement with the results of the band spectrum calculations; however, all investigations were carried out only for the ΓL direction.

Other methods involving laser diffraction in structural studies of colloidal crystals are available. For example, the dependences of the reflection intensity at a fixed angle of incidence for different positions of detector were plotted and conclusions about the structure of the sample were made based on the peak positions and broadening.[243] The shape and features of the behaviour of defects in colloidal crystals were determined by studying the fine structure of diffraction reflections (small spots constituting the reflection).[244–246] The diffraction pattern was used to determine the orientation of a region of an inverse opal film, on which the laser beam was focussed.[139] Scanning of the sample was followed by constructing the orientation maps for different domains. When the spot of the laser beam reached a two- or tri-domain region, a superposition of diffraction patterns from different domains was observed (Fig. 10).

5. Analysis of Kossel ring patterns

Yet another widely used method of investigation of the structure of colloidal crystals is an analysis of Kossel ring patterns. The essence of the method is as follows. As diffuse laser radiation propagates through a periodic structure, diffraction from different crystal planes causes a significant decrease in its intensity. As a result, one gets a pattern with dark lines called the Kossel ring patterns whose shape and positions allow the opal structure to be analyzed.[247, 248]

The Kossel ring patterns obtained for a colloidal crystal based on polystyrene spheres in water are shown in Fig. 11.[243] The central circumference in Fig. 11 *b* corresponds to the second order diffraction from the (111) planes of the fcc structure; other Kossel ring patterns are due to diffraction from the {220} families of planes. The observed sixfold axis for the {220} rings instead of a threefold axis expected for the fcc structure corresponds to twinning in the sample. Note that the method requires good transmission of radiation through the opal; therefore, it can be used only in studies of colloidal crystals with low optical contrast.[249–253]

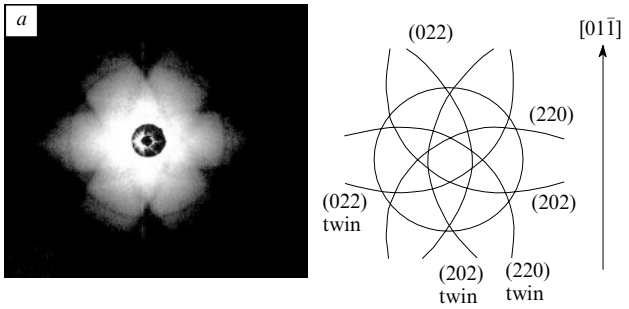


Figure 11. The Kossel ring pattern at normal incidence of laser radiation (λ = 488 nm, lattice constant is 766 nm) on the (111) plane of a colloidal crystal (*a*) and schematic view of the lines obtained (*b*).[243]

VI. Conclusion

At present, the structure of photonic crystals can be controlled by various methods. Among them, microradian X-ray diffraction seems to be the most informative; electron microscopy provides clear images; optical (laser) diffraction is a quick technique for studying structures whose lattice constants are larger than the wavelength of light used.

Structural imperfection of opaline materials is the main problem related to their operation. The method of vertical deposition allows one to obtain opal films with rather large highly ordered surface areas; however, such abundant distortions of the periodic structure as the size dispersion of spherical microparticles and stacking faults, strongly affect their optical properties. At the same time, requirements for the quality of the structure of photonic crystals in some cases differ significantly. In this connection, one may state the following.

If there is a need for a complete photonic band gap, high concentrations of defects producing uncontrolled levels within this band gap may appear to be inappropriate. Taking into account the fact that the photonic band gap opens in the high-index regions of the band spectra of inverse opals (provided that the optical contrast of the structure is high enough), stacking faults may appear to be of particular importance. These defects strongly affect the high-index bands but have little effect on the first photonic stop band in the region of the L-point of the Brillouin zone.

Displacements of microspheres from ideal positions as well as other defects are the reason for strong scattering of light from synthetic opals; this precludes control of light fluxes within these systems. At the same time, this factor becomes much less important (and opal transparency increases) as the optical contrast of the structure decreases; this can be attained by introducing a corresponding filler. For the same reasons it is desired to use opal photonic crystals for control of reflected rather than transmitted beams.

Finally, these are some fields of application for which structural defects in opals are by and large insignificant although undesired. These include enhancement of nonlinear optical, magnetooptical, photoelectric, photocatalytic and other effects related to the interaction of light with matter [5] due to the Bragg diffraction and slowing down the group velocity of light at the boundaries of the stop bands. Possible influence of defects on the group velocity of light is still to be clarified, but it is assumed that most defects have little effect on this parameter. Taking into account the fact that synthetic opals still remain the most available for the visible region, cheap and readily producible photonic crys-

tals having no limitation on the linear dimensions, one can assume that they will find a wide range of applications for these purposes in the nearest future.

References

1. V N Astratov, V N Bogomolov, A A Kaplyanskii, A V Prokofiev, L A Samoilovich, S M Samoilovich, Yu A Vlasov *Nuovo Cimento D* **17** 1349 (1995)
2. C López *Adv. Mater.* **15** 1679 (2003)
3. C López *Adv. Mater.* **23** 30 (2011)
4. O D Velev, S Gupta *Adv. Mater.* **21** 1897 (2009)
5. F Marlow, Muldarisnur, P Sharifi, R Brinkmann, C Mendive *Ang. Chem., Int. Ed.* **48** 6212 (2009)
6. J H Moon, S Yang *Chem. Rev.* **110** 547 (2010)
7. E Yablonovitch *Phys. Rev. Lett.* **58** 2059 (1987)
8. S John *Phys. Rev. Lett.* **58** 2486 (1987)
9. V P Bykov *Zh. Eksp. Teor. Fiz.* **62** 505 (1972) [a]
10. V P Bykov *Dokl. Akad. Nauk SSSR* **205** 60 (1972) [b]
11. V P Bykov *Kvant. Elektron.* **1** 1557 (1974) [c]
12. A Blanco, E Chomski, S Grabtchak, M Ibisate, S John, S W Leonard, C Lopez, F Meseguer, H Miguez, J P Mondia, G A Ozin, O Toader, H M van Driel *Nature (London)* **405** 437 (2000)
13. T F Krauss, R M De La Rue *Prog. Quant. Electron.* **23** 51 (1999)
14. E Matioli, C Weisbuch *J. Phys. D* **43** 354005 (2010)
15. S Lin, E Chow, V Hietala, P R Villeneuve, J D Joannopoulos *Science* **282** 274 (1998)
16. R F Cregan, B J Mangan, J C Knight, T A Birks, P St J Russell, P J Roberts, D C Allan *Science* **285** 1537 (1999)
17. S G Johnson, J D Joannopoulos *Acta Mater.* **51** 5823 (2003)
18. S A Rinne, F Garcia-Santamaria, P V Braun *Nature Photon.* **2** 52 (2008)
19. O Painter, R K Lee, A Scherer, A Yariv, J D O'Brien, P D Dapkus, I Kim *Science* **284** 1819 (1999)
20. M Loncar, T Yoshie, A Scherer, P Gogna, Y Qiu *Appl. Phys. Lett.* **81** 2680 (2002)
21. M N Shkunov, M C DeLong, M E Raikh, Z V Vardeny, A A Zakhidov, R P Baughman *Synth. Met.* **116** 485 (2001)
22. G A Emelchenko, A N Gruzintsev, V T Volkov, V M Masalov, A V Bazhenov, D A Fokin *Photon. Nanostruct. Fund. Appl.* **5** 96 (2007)
23. O K Alimov, T T Basiev, Yu V Orlovskii, V V Osiko, M I Samoilovich *Kvant. Elektron.* **38** 665 (2008) [c]
24. M Meier, A Mekis, A Dodabalapur, A Timko, R E Slusher, J D Joannopoulos, O Nalamasu *Appl. Phys. Lett.* **74** 7 (1999)
25. M Scharrer, A Yamilov, X Wu, H Cao, R P H Chang *Appl. Phys. Lett.* **88** 201103 (2006)
26. M Inoue, K Arai, T Fujii, M Abe *J. Appl. Phys.* **83** 6768 (1998)
27. M Inoue, K Arai, T Fujii, M Abe *J. Appl. Phys.* **85** 5768 (1999)
28. A A Grunin, A G Zhdanov, A A Ezhov, E A Ganshina, A A Fedyanin *Appl. Phys. Lett.* **97** 261908 (2010)
29. V I Belotelov, I A Akimov, M Pohl, V A Kotov, S Kasture, A S Vengurlekar, Achanta Venu Gopal, D R Yakovlev, A K Zvezdin, M Bayer *Nature Nanotechnol.* **6** 370 (2011)
30. T V Murzina, E M Kim, R V Kapra, I V Moshnina, O Aktsipetrov, D A Kurdyukov, S F Kaplan, V G Golubev, M A Bader, G Marowsky *Appl. Phys. Lett.* **88** 022501 (2006)
31. V V Pavlov, P A Usachev, R V Pisarev, D A Kurdyukov, S F Kaplan, A V Kimel, A Kirilyuk, Th Rasing *Appl. Phys. Lett.* **93** 072502 (2008)
32. K Napolskii, N Sapoletova, A Eliseev, G Tsirlina, A Rubacheva, E Gan'shina, M Kuznetsov, M Ivanov, V Valdner, E Mishina, A van Ettegerc, Th Rasing *J. Magn. Magn. Mater.* **321** 833 (2008)
33. P P Markowicz, H Tiryaki, H Pudavar, P N Prasad, N N Lepeshkin, R W Boyd *Phys. Rev. Lett.* **92** 083903 (2004)
34. A A Fedyanin, O Aktsipetrov, D A Kurdyukov, V G Golubev *Appl. Phys. Lett.* **87** 151111 (2005)
35. J I L Chen, G von Freymann, S Y Choi, V Kitaev, G A Ozin *Adv. Mater.* **18** 1915 (2006)
36. H Kosaka, T Kawashima, A Tomita, M Notomi, T Tamamura, T Sato, S Kawakami *Phys. Rev. B* **58** R10096 (1998)
37. M Notomi *Phys. Rev. B* **62** 10696 (2000)
38. S G Romanov, T Maka, C M S Torres, M Müller, R Zentel *Synth. Met.* **124** 131 (2001)
39. A F Koenderink, W L Vos *Phys. Rev. Lett.* **91** 213902 (2003)
40. I S Nikolaev, P Lodahl, W L Vos *Phys. Rev. A* **71** 053813 (2005)
41. S F Kaplan, N F Kartenko, D A Kurdyukov, A V Medvedev, V G Golubev *Appl. Phys. Lett.* **86** 071108 (2005)
42. M Li, P Zhang, J Li, J Zhou, A Sinitskii, V Abramova, S O Klimonskii, Y D Tretyakov *Appl. Phys. B* **89** 251 (2007)
43. A S Sinitskii, S O Klimonskii, S V Eliseeva, Yu D Tretyakov, Zh Li, P Chzhang, M Li, Zh I Chzhou *Pis'ma v Zh. Eksp. Teor. Fiz.* **87** 772 (2008) [d]
44. E Yablonovitch, T J Gmitter, K M Leung *Phys. Rev. Lett.* **67** 2295 (1991)
45. S Noda, K Tomoda, N Yamamoto, A Chutinan *Science* **289** 604 (2000)
46. J G Fleming, S Y Lin, I El-Kady, R Biswas, K M Ho *Nature (London)* **417** 52 (2002)
47. K M Leung, Y F Liu *Phys. Rev. Lett.* **65** 2646 (1990)
48. H S Sözüer, J W Haus, R Inguva *Phys. Rev. B* **45** 13962 (1992)
49. K Busch, S John *Phys. Rev. E* **58** 3896 (1998)
50. K M Ho, C T Chan, C M Soukoulis *Phys. Rev. Lett.* **65** 3152 (1990)
51. M Maldovan, E L Thomas *Nature Mater.* **3** 593 (2004)
52. M J Escuti, G P Crawford *Opt. Eng.* **43** 1973 (2004)
53. V Ramanan, E Nelson, A Brzezinsky, P V Braun, P Wiltzius *Appl. Phys. Lett.* **92** 173304 (2008)
54. J Li, Y Liu, X Xie, P Zhang, B Liang, Li Yan, J Zhou, G Kurizki, D Jacobs, K S Wong, Y Zhong *Opt. Express* **16** 12899 (2008)
55. J Li, B Liang, Y Liu, P Zhang, J Zhou, S O Klimonsky, A S Slesarev, Yu D Tretyakov, L O'Faolain, T F Krauss *Adv. Mater.* **22** 2676 (2010)
56. N D Deniskina, D V Kalinin, L K Kazantseva *Blagorodnye Opaly, ikh Sintez i Genezis v Prirode* (Noble Opals, Their Synthesis and Genesis in Nature) (Novosibirsk: Nauka, 1980)
57. J V Sanders *Nature (London)* **204** 1151 (1964)
58. US P. 3497367; *Chem. Abstr.* **72** 113342t (1970)
59. N I Kornilov, Yu P Solodova *Yuvelirnye Kamni* (Jewelry Stones) (Moscow: Nedra, 1982)
60. W Stöber, A Fink, E Bohn *J. Colloid Interface Sci.* **26** 62 (1968)
61. G H Bogush, M A Tracy, C F Zukoski *J. Non-Cryst. Solids* **104** 95 (1988)
62. D W McComb, B M Treble, C J Smith, R M De La Rue, N P Johnson *J. Mater. Chem.* **11** 142 (2001)
63. V M Masalov, K A Aldushin, P V Dolganov, G A Emel'chenko *Phys. Low-Dimens. Struct.* **5**–**6** 45 (2001)
64. T Yokoi, Y Sakomoto, O Teresaki, Y Kubota, T Okubo, T Tatsumi *J. Am. Chem. Soc.* **128** 13664 (2006)
65. K D Hartlen, A P T Athanasopoulos, V Kitaev *Langmuir* **24** 1714 (2008)
66. D A S Razo, L Pallavidino, E Garrone, F Geobaldo, E Descrovi, A Chiodoni, F Giorgis *J. Nanopart. Res.* **10** 1225 (2008)
67. J W Goodwin, J Hearn, C C Ho, R H Ottewill *Colloid Polym. Sci.* **252** 464 (1974)
68. K Tauer, R Deckwer, I Kühn, C Schellenberg *Colloid Polym. Sci.* **277** 607 (1999)
69. C E Reese, S A Asher *J. Colloid Interface Sci.* **248** 41 (2002)

70. A Yu Menshikova, B M Shabsels, N N Shevchenko, A G Bazhenova, A B Pevtsov, A V Sel'kin, A Yu Bilibin *Colloids Surf., A* **298** 27 (2007)
71. A Yu Men'shikova *Ros. Nanotekhnol.* **5** (1 – 2) 52 (2010) [e]
72. A S Sinitskii, A V Knot'ko, Yu D Tretyakov *Neorg. Mater.* **41** 1336 (2005) [f]
73. A Stein *Microporous Mesoporous Mater.* **44** – **45** 227 (2001)
74. N P Johnson, D W McComb, A Richel, M Treble, R M De La Rue *Synth. Met.* **116** 469 (2001)
75. M Holgado, F Garcia-Santamaria, A Blanco, M Ibisate, A Cintas, H Miguez, C J Serna, C Molpeceres, J Requena, A Mifsud, F Meseguer, C López *Langmuir* **15** 4701 (1999)
76. O D Velev, T A Jede, R F Lobo, A M Lenhoff *Chem. Mater.* **10** 3597 (1998)
77. O D Velev, P M Tessier, A M Lenhoff, E W Kaler *Nature (London)* **401** 548 (1999)
78. P Jiang, J F Bertone, K S Hwang, V Colvin *Chem. Mater.* **11** 2132 (1999)
79. J F Bertone, P Jiang, K S Hwang, D M Mittleman, V L Colvin *Phys. Rev. Lett.* **83** 300 (1999)
80. A S Dimitrov, K Nagayama *Langmuir* **12** 1303 (1996)
81. A S Dimitrov, T Miwa, K Nagayama *Langmuir* **15** 5257 (1999)
82. K Wostyn, Y Zhao, B Yee, K Clays, A Persoons, G de Schaetzen, L Hellemans *J. Chem. Phys.* **118** 10752 (2003)
83. Yu A Vlasov, X-Z Bo, J C Sturm, D J Norris *Nature (London)* **414** 289 (2001)
84. S Wong, V Kitaev, G A Ozin *J. Am. Chem. Soc.* **125** 15589 (2003)
85. K S Napolskii, N A Sapoletova, D F Gorozhankin, A A Eliseev, D Yu Chernyshov, D V Byelov, N A Grigoryeva, A A Mistonov, W G Bouwman, K O Kvashnina, A V Lukashin, A A Snigirev, A V Vasilieva, S V Grigoriev, A V Petukhov *Langmuir* **26** 2346 (2010)
86. Y-H Ye, F LeBlanc, A Hache, V-V Truong *Appl. Phys. Lett.* **78** 52 (2001)
87. M McLachlan, N Johnson, R De La Rue, D McComb *J. Mater. Chem.* **14** 144 (2004)
88. S-L Kuai, X-F Hub, A Hache, V-V Truong *J. Cryst. Growth* **267** 317 (2004)
89. M McLachlan, N Johnson, R De La Rue, D McComb *J. Mater. Chem.* **15** 369 (2005)
90. S H Im, M H Kim, O O Park *Chem. Mater.* **15** 1797 (2003)
91. H-L Li, F Marlow *Chem. Mater.* **18** 1803 (2006)
92. F Piret, B-L Su *Chem. Phys. Lett.* **457** 376 (2008)
93. S H Im, Y T Lim, D J Suh, O O Park *Adv. Mater.* **14** 1367 (2002)
94. Y Xu, G J Schneider, E D Wetzel, D W Prather *J. Microlith., Microfab. Microsyst.* **3** 168 (2004)
95. S H Park, Y Xia *Chem. Mater.* **10** 1745 (1998)
96. S H Park, D Qin, Y Xia *Adv. Mater.* **10** 1028 (1998)
97. S H Park, Y Xia *Adv. Mater.* **10** 1045 (1998)
98. G Pan, R Kesavamoorthy, S A Asher *Phys. Rev. Lett.* **78** 3860 (1997)
99. G Pan, R Kesavamoorthy, S A Asher *J. Am. Chem. Soc.* **120** 6525 (1998)
100. S-H Kim, Se-H Kim, W C Jeong, S-M Yang *Chem. Mater.* **21** 4993 (2009)
101. S-H Kim, H S Park, J H Choi, J W Shim, S-M Yang *Adv. Mater.* **22** 946 (2010)
102. Y Xia, B Gates, Y Yin, Y Lu *Adv. Mater.* **12** 693 (2000)
103. L Xu, W L Zhou, C Frommen, R H Baughman, A A Zakhidov, L Malkinski, J-Q Wang, J B Wiley *Chem. Commun.* 997 (2000)
104. P N Bartlett, P R Birkin, M A Ghanem *Chem. Commun.* 1671 (2000)
105. H Yan, C F Blanford, B T Holland, M Parent, W H Smyrl, A Stein *Adv. Mater.* **11** 1003 (1999)
106. A A Zakhidov, R H Baughman, I I Khayrullin, I A Udod, M Kozlov, N Eradat, V Z Vardeny, M Sigalas, R Biswas *Synth. Met.* **116** 419 (2001)
107. J E G J Wijnhoven, S J M Zevenhuizen, M A Hendriks, D Vanmaekelbergh, J J Kelly, W L Vos *Adv. Mater.* **12** 888 (2000)
108. P Jiang, J Cizeron, J F Bertone, V L Colvin *J. Am. Chem. Soc.* **121** 7957 (1999)
109. P N Bartlett, J J Baumberg, P R Birkin, M A Ghanem, M C Netti *Chem. Mater.* **14** 2199 (2002)
110. P N Bartlett, M A Ghanem, I S El Hallag, P de Groot, A Zhukov *J. Mater. Chem.* **13** 2596 (2003)
111. B H Juárez, C López, C Alonso *J. Phys. Chem. B* **108** 16708 (2004)
112. X Yu, Y J Lee, R Furstenberg, J O White, P V Braun *Adv. Mater.* **19** 1689 (2007)
113. K S Napolskii, A Sinitskii, S V Grigoriev, N A Grigorieva, H Eckerlebe, A A Eliseev, A V Lukashin, Yu D Tretyakov *Physica B* **397** 23 (2007)
114. S V Grigoriev, K S Napolskii, N A Grigoryeva, A V Vasilieva, A A Mistonov, D Yu Chernyshov, A V Petukhov, D V Belov, A A Eliseev, A V Lukashin, Yu D Tretyakov, A S Sinitskii, H Eckerlebe *Phys. Rev. B* **79** 045123 (2009)
115. A A Zakhidov, R H Baughman, Z Iqbal, C Cui, I Khayrullin, S O Dantas, J Marti, V G Ralchenko *Science* **282** 897 (1998)
116. N Tétreault, H Míguez, G A Ozin *Adv. Mater.* **16** 1471 (2004)
117. H Míguez, F Meseguer, C López, M Holgado, G Andreasen, A Mifsud, V Fornés *Langmuir* **16** 4405 (2000)
118. H Míguez, E Chomski, F García-Santamarta, M Ibisate, S John, C López, F Meseguer, J P Mondia, G A Ozin, O Toader, H M van Driel *Adv. Mater.* **13** 1634 (2001)
119. F Meseguer, A Blanco, H Míguez, F García-Santamarta, M Ibisate, C López *Colloids Surf., A* **202** 281 (2002)
120. J E G J Wijnhoven, W L Vos *Science* **281** 802 (1998)
121. B T Holland, C F Blanford, A Stein *Science* **281** 538 (1998)
122. B T Holland, C F Blanford, T Do, A Stein *Chem. Mater.* **11** 795 (1999)
123. G Subramanian, K Constant, R Biswas, M M Sigalas, K M Ho *Appl. Phys. Lett.* **74** 3933 (1999)
124. G Subramanian, V N Monoharan, J D Thorne, D J Pine *Adv. Mater.* **11** 1261 (1999)
125. H Yan, C F Blanford, B T Holland, W H Smyrl, A Stein *Chem. Mater.* **12** 1134 (2000)
126. Z-Z Gu, S Hayami, S Kubo, Q-B Meng, Y Einaga, D A Tryk, A Fujishima, O Sato *J. Am. Chem. Soc.* **123** 175 (2001)
127. P Jiang, J F Bertone, V L Colvin *Science* **291** 453 (2001)
128. J E G J Wijnhoven, L Bechger, W L Vos *Chem. Mater.* **13** 4486 (2001)
129. A Richel, N P Johnson, D W McComb *Appl. Phys. Lett.* **76** 1816 (2000)
130. B Gates, B Mayers, Z-Y Li, Y Xia *Mater. Res. Soc. Symp. Proc.* **636** D9.15.1 (2001)
131. Z-Z Gu, S Kubo, A Fujishima, O Sato *Appl. Phys. A* **74** 127 (2002)
132. S-L Kuai, X F Hu, V-V Troung *J. Cryst. Growth* **259** 404 (2003)
133. S-L Kuai, V-V Troung, A Hache, X-F Hu *J. Appl. Phys.* **96** 5982 (2004)
134. L I Halaoui, N M Abrams, T E Mallouk *J. Chem. Phys. B* **109** 6334 (2005)
135. S Badilescu, P V Ashrit *Solid State Ionics* **158** 187 (2003)
136. S-L Kuai, G Bader, P V Ashrit *Appl. Phys. Lett.* **86** 221110 (2005)
137. V G Golubev, V Yu Davydov, N F Kartenko, D A Kurdyukov, A V Medvedev, A B Pevtsov, A V Scherbakov, E B Shadrin *Appl. Phys. Lett.* **79** 2127 (2001)

138. D A Mazurenko, R Kerst, J I Dijkhuis, A V Akimov, V G Golubev, A A Kaplyanskii, D A Kurdyukov, A B Pevtsov *Appl. Phys. Lett.* **86** 041114 (2005)
139. A Sinitskii, V Abramova, T Laptinskaya, Yu Tretyakov *Phys. Lett. A* **366** 516 (2007)
140. V V Abramova, A S Sinitskii, Yu D Tretyakov *Pis'ma Zh. Exp. Theor. Fiz.* **86** 370 (2007) [d]
141. A S Sinitskii, V V Abramova, Yu D Tretyakov *Mendeleev Commun.* **17** 1 (2007)
142. A Sinitskii, V Abramova, T Laptinskaya, Yu Tretyakov *Superlatt. Microstruct.* **44** 626 (2008)
143. V Abramova, A Sinitskii *Superlatt. Microstruct.* **45** 624 (2009)
144. A Sinitskii, V Abramova, N Grigorieva, S Grigoriev, A Snigirev, D V Byelov, A V Petukhov *Europhys. Lett.* **89** 14002 (2010)
145. L Li, U Steiner, S Mahajan *J. Mater. Chem.* **20** 7131 (2010)
146. Y Li, F Piret, T Lgonard, B-L Su *J. Colloid Interface Sci.* **348** 43 (2010)
147. W Liu, B Zou, J Zhao, H Cui *Thin Solid Films* **518** 4923 (2010)
148. Q Liu, H Song, W Wang, X Bai, Yu Wang, B Dong, L Xu, W Han *Opt. Lett.* **35** 2898 (2010)
149. X Qu, H K Yang, B K Moon, B C Choi, J H Jeong, K H Kim *J. Phys. Chem. C* **114** 19891 (2010)
150. D J Norris, Yu A Vlasov *Adv. Mater.* **13** 371 (2001)
151. P V Braun, P Wiltzius *Nature (London)* **402** 603 (1999)
152. Yu A Vlasov, N Yao, D J Norris *Adv. Mater.* **11** 165 (1999)
153. S G Romanov, T Maka, C M Sotomayor Torres, M Müller, R Zentel *Appl. Phys. Lett.* **79** 731 (2001)
154. V G Golubev, J L Hutchison, V A Kosobukin, D A Kurdyukov, A V Medvedev, A B Pevtsov, J Sloan, L M Sorokin *J. Non-Cryst. Solids* **299** – **302** 1062 (2002)
155. S G Romanov, R M De La Rue, H M Yates, M E Pemble *J. Phys.: Condens. Matter* **12** 339 (2000)
156. G Gajiev, V G Golubev, D A Kurdyukov, A B Pevtsov, A V Selkin, V V Travnikov *Phys. Status Solidi, B* **231** R7 (2002)
157. D A Kurdyukov, N F Kartenko, V G Golubev *J. Alloys Compd.* **492** 611 (2010)
158. S A Johnson, P J Ollivier, T E Mallouk *Science* **283** 963 (1999)
159. J Li, Y Wu, J Fu, Y Cong, J Peng, Y Han *Chem. Phys. Lett.* **390** 285 (2004)
160. H Fudouzi, T Sawada *Langmuir* **22** 1365 (2006)
161. A C Arsenault, T J Clark, G von Freymann, L Cademartiri, R Sapienza, J Bertolotti, E Vekris, S Wong, V Kitaev, I Manners, R Z Wang, S John, D Wiersma, G A Ozin *Nature Mater.* **5** 179 (2006)
162. V N Bogomolov, T M Pavlova *Fiz. Tekhn. Poluprovodnikov* **29** 826 (1995) [g]
163. D A Kurdyukov *Nanotekhnika* **4** 18 (2007)
164. S G Romanov, N P Johnson, A V Fokin, V Y Butko, H M Yates, M E Pemble, C M Torres Sotomayor *Appl. Phys. Lett.* **70** 2091 (1997)
165. H M Yates, M E Pemble, H Miguez, A Blanco, C López, F Meseguer, L Vázquez *J. Cryst. Growth* **193** 9 (1998)
166. S Fan, P R Villeneuve, J D Joannopoulos *Phys. Rev. B* **54** 11245 (1996)
167. A Moroz *Phys. Rev. Lett.* **83** 5274 (1999)
168. W Y Zhang, X Y Lei, Z L Wang, D G Zheng, W Y Tam, C T Chan, P Sheng *Phys. Rev. Lett.* **84** 2853 (2000)
169. I El-Kady, M M Sigalas, R Biswas, K M Ho, C M Soukoulis *Phys. Rev. B* **62** 15299 (2000)
170. P V Braun, P Wiltzius *Adv. Mater.* **13** 482 (2001)
171. T Sumida, Y Wada, T Kitamura, S Yanagida *Chem. Lett.* **30** 38 (2001)
172. Y-J Huang, C-H Liao, B-H Huang, W-Y Chen, P-W Wu *J. Electrochem. Soc.* **158** (4) P45 (2011)
173. P Pusey, W van Megen, P Bartlett, B Ackerson, J Rarity, S Underwood *Phys. Rev. Lett.* **63** 2753 (1989)
174. J Zhu, M Li, R Rogers, W Meyer, R H Ottewill, W B Russel, STS-73 Space Shuttle Crew, P M Chaikin *Nature (London)* **387** 883 (1997)
175. S Sastry, T M Truskett, P G Debenedetti, S Torquato, F H Stillinger *Mol. Phys.* **95** 289 (1998)
176. L V Woodcock *Nature (London)* **385** 141 (1997)
177. H Miguez, F Meseguer, C López, A Mifsud, J S Moya, L Vázquez *Langmuir* **13** 6009 (1997)
178. Yu A Vlasov, V N Astratov, A V Baryshev, A A Kaplyanskii, O Z Karimov, M F Limonov *Phys. Rev. E* **61** 5784 (2000)
179. Yu A Vlasov, M Deutsch, D J Norris *Appl. Phys. Lett.* **76** 1627 (2000)
180. A S Sinitskii, P E Khokhlov, V V Abramova, T V Laptinskaya, Yu D Tretyakov *Mendeleev Commun.* **17** 4 (2007)
181. J Hilhorst, V V Abramova, A Sinitskii, N A Sapoletova, K S Napolskii, A A Eliseev, D V Byelov, N A Grigoryeva, A V Vasilieva, W G Bouwman, K Kvashnina, A Snigirev, S V Grigoriev, A V Petukhov *Langmuir* **25** 10408 (2009)
182. J F Galisteo-López, E Palacios-Lidón, E Castillo-Martínez, C López *Phys. Rev. B* **68** 115109 (2003)
183. S G Romanov, T Maka, C M Sotomayor Torres, M Müller, R Zentel, D Cassagne, J Manzanares-Martinez, C Jouanin *Phys. Rev. E* **63** 056603 (2001)
184. D J Norris, E Arlinghaus, L Meng, R Heiny, L Scriven *Adv. Mater.* **16** 1393 (2004)
185. L Meng, H Wei, A Nagel, B Wiley, L Scriven, D J Norris *Nano Lett.* **6** 2249 (2006)
186. S P Molchanov, P V Lebedev-Stepanov, S O Klimonsky, K F Sheberstov, S Yu Tretyakov, M V Alfimov *Ros. Nanotekhnol.* **5** (5 – 6) 18 (2010) [e]
187. L C Andreani, A Balestreri, J F Galisteo-López, M Galli, M Patrini, E Descrovi, A Chiodoni, F Giorgis, L Pallavidino, F Geobaldo *Phys. Rev. B* **78** 205304 (2008)
188. A A Chabanov, Y Jun, D J Norris *Appl. Phys. Lett.* **84** 3573 (2004)
189. T Sumida, Y Wada, T Kitamura, S Yanagida *Langmuir* **18** 3886 (2002)
190. Z Wang, C Chan, W Zhang, Z Chen, N Ming, P Sheng *Phys. Rev. E* **67** 016612 (2003)
191. R Rengarajan, D Mittleman, C Rich, V Colvin *Phys. Rev. E* **71** 016615 (2005)
192. A F Koenderink, M Megens, G van Soest, W LVos, A Lagendijk *Phys. Lett. A* **268** 104 (2000)
193. B Gates, Y Xia *Appl. Phys. Lett.* **78** 3178 (2001)
194. E Palacios-Lidón, B Juárez, E Castillo-Martínez, C López *J. Appl. Phys.* **97** 063502 (2005)
195. I A Karpov, E N Samarov, V M Masalov, S I Bozhko, G A Emel'chenko *Fiz. Tv. Tela* **47** 334 (2005) [h]
196. I I Bardyshev, A D Mokrushin, A A Pribylov, E N Samarov, V M Masalov, I A Karpov, G A Emel'chenko *Kolloid. Zh.* **68** 25 (2006) [i]
197. V M Masalov, N S Sukhinina, E A Kudrenko, G A Emelchenko *Nanotechnology* **22** 275718 (2011)
198. A V Baryshev, A B Khanikaev, M Inoue, P B Lim, A V Sel'kin, G Yushin, M F Limonov *Phys. Rev. Lett.* **99** 063906 (2007)
199. M V Rybin, A V Baryshev, A B Khanikaev, M Inoue, K B Samusev, A V Sel'kin, G Yushin, M F Limonov *Phys. Rev. B* **77** 205106 (2008)
200. A K Samusev, M V Rybin, M F Limonov *Fiz. Tv. Tela* **51** 487 (2009) [h]
201. A K Samusev, K B Samusev, M V Rybin, M F Limonov *J. Phys.: Condens. Matter* **22** 115401 (2010)
202. N A M Verhaegh, J S van Duijneveldt, A van Blaaderen, H N W Lekkerkerker *J. Chem. Phys.* **102** 1416 (1995)

203. H Wei, L Meng, Y Jun, D J Norris *Appl. Phys. Lett.* **89** 241913 (2006)
204. G Lozano, H Mtguez *Appl. Phys. Lett.* **92** 091904 (2008)
205. J F Galisteo-López, M Galli, M Patrini, A Balestreri, L C Andreani, C López *Phys. Rev. B* **73** 125103 (2006)
206. L A Dorado, R A Depine, H Míguez *Phys. Rev. B* **75** R241101 (2005)
207. K B Samusev, A V Baryshev, A A Kaplyanskii, V A Kosobukin, D E Usvyat, M F Limonov *Phys. Rev. B* **70** 113104 (2004)
208. H J Schöpe, A B Fontecha, H König, J M Hueso, R Biehl *Langmuir* **22** 1828 (2006)
209. X Checoury, S Enoch, C López, A Blanco *Appl. Phys. Lett.* **90** 161131 (2007)
210. E Vekris, V Kitaev, D Perovic, J S Aitchison, G A Ozin *Adv. Mater.* **20** 1110 (2008)
211. C Kittel *Introduction to Solid State Physics* (8th Ed.) (New York: Wiley, 2004)
212. A Guinier *X-Ray Diffraction in Crystals, Imperfect Crystals and Amorphous Bodies* (San Francisco: Freeman, 1963)
213. C F Bohren, D R Huffman *Absorption and Scattering of Light by Small Particles* (New York: Wiley, 1983)
214. A J C Wilson *X-Ray Optics* (London: Methuen, 1962)
215. W Loose, B J Ackerson *J. Chem. Phys.* **101** 7211 (1994)
216. A V Petukhov, D G A L Aarts, I P Dolbnya, E H A de Hoog, K Kassapidou, G J Vroege, W Bras, H N W Lekkerkerker *Phys. Rev. Lett.* **88** 208301 (2002)
217. B J Ackerson, J B Hayter, N A Clark, L Cotter *J. Chem. Phys.* **84** 2344 (1986)
218. S Ashdown, I Marcović, R H Ottewill, P Lindner, R C Oberthür, A R Rennie *Langmuir* **6** 303 (1990)
219. H M Laun, R Bung, S Hess, W Loose, O Hess, K Hahn, E Hadicke, R Hingmann, F Schmidt *J. Rheol.* **36** 743 (1992)
220. H Versmold, P Lindner *Langmuir* **10** 3043 (1994)
221. H Versmold *Phys. Rev. Lett.* **75** 763 (1995)
222. W L Vos, M Megens, C M van Kats, P Bösecke *Langmuir* **13** 6004 (1997)
223. A V Petukhov, I P Dolbnya, D G A L Aarts, G J Vroege, H N W Lekkerkerker *Phys. Rev. Lett.* **90** 028304 (2003)
224. X Xian, A V Petukhov, M M E Snel, I P Dolbnya, D G A L Aarts, G J Vroege, H N W Lekkerkerker *J. Appl. Crystallogr.* **36** 597 (2003)
225. A V Petukhov, I P Dolbnya, D G A L Aarts, G J Vroege *Phys. Rev. E* **69** 031405 (2004)
226. I P Dolbnya, A V Petukhov, D G A L Aarts, G J Vroege, H N W Lekkerkerker *Europhys. Lett.* **72** 962 (2005)
227. A V Petukhov, J H J Thijssen, D C t'Hart, A Imhof, A van Blaaderen, I P Dolbnya, A A Snigirev, A Moussaid, A Snigireva *J. Appl. Crystallogr.* **39** 137 (2006)
228. J H J Thijssen, A V Petukhov, D C t'Hart, A Imhof, C H M van der Werf, R E I Schropp, A van Blaaderen *Adv. Mater.* **18** 1662 (2006)
229. V V Abramova, A S Sinitskii, N A Grigor'eva, S V Grigor'ev, D V Belov, A V Petukhov, A A Mistonov, A V Vasil'eva, Yu D Tretyakov *Zh. Eksp. Teor. Fiz.* **136** 37 (2009) [a]
230. A A Eliseev, D F Gorozhankin, K S Napol'skii, A V Petukhov, N A Sapoletova, A V Vasil'eva, N A Grigor'eva, A A Mistonov, D V Belov, V G Bauman, K O Kvashnina, D Yu Chernyshev, A A Bosak, S V Grigor'ev *Pis'ma Zh. Eksp. Teor. Fiz.* **90** 297 (2009) [d]
231. B J Ackerson, N A Clark *Phys. Rev. Lett.* **46** 123 (1981)
232. W K Kegel, J K G Dhont *J. Chem. Phys.* **112** 3431 (2000)
233. V C Martelozzo, A B Schofield, W C K Poon, P N Pusey *Phys. Rev. E* **66** 021408 (2002)
234. T Yamasaki, T Tsutsui *Jpn. J. Appl. Phys.* **38** 5916 (1999)
235. R Amos, J Rarity, P Tapster, T Shepherd, S Kitson *Phys. Rev. E* **61** 2929 (2000)
236. L Goldenberg, J Wagner, J Stumpe, B Paulke, E Görnitz *Langmuir* **18** 3319 (2002)
237. S O Lumsdon, E W Kaler, J P Williams, O D Velev *Appl. Phys. Lett.* **82** 949 (2003)
238. B G Prevo, O D Velev *Langmuir* **20** 2099 (2004)
239. M Allard, E H Sargent, P C Lewis, E Kumacheva *Adv. Mater.* **16** 1360 (2004)
240. J Sun, Y Li, H Dong, P Zhan, C Tang, M Zhu, Z Wang *Adv. Mater.* **20** 123 (2008)
241. C Dux, H Versmold *Phys. Rev. Lett.* **78** 1811 (1997)
242. F García-Santamaría, J F Galisteo-López, P Braun, C López *Phys. Rev. B* **71** 195112 (2005)
243. S Asher, J Weissman, A Tikhonov, R Coalson, R Kesavamoorthy *Phys. Rev. E* **69** 066619 (2004)
244. J Liu, D A Weitz, B J Ackerson *Phys. Rev. E* **48** 1106 (1993)
245. P Schall, I Cohen, D A Weitz, F Spaepen *Science* **305** 1944 (2004)
246. P Schall, I Cohen, D A Weitz, F Spaepen *Nature (London)* **440** 319 (2006)
247. T Yoshiyama, I Sogami *Phys. Rev. Lett.* **53** 2153 (1984)
248. T Yoshiyama, I Sogami *Phys. Rev. Lett.* **56** 1609 (1986)
249. R D Pradhan, J A Bloodgood, G H Watson *Phys. Rev. Lett.* **55** 9503 (1997)
250. T Shinohara, T Yoshiyama, I S Sogami, T Konishi, N Ise *Langmuir* **17** 8010 (2001)
251. T Kanai, T Sawada, I Maki, K Kitamura *Jpn. J. Appl. Phys.* **42** L655 (2003)
252. T Shinohara, H Yamada, I S Sogami, N Ise, T Yoshiyama *Langmuir* **20** 5141 (2004)
253. T Shinohara, T Kurokawa, T Yoshiyama, T Itoh, I Sogami, N Isei *Phys. Rev. E* **70** 062401 (2004)

[a] — *J. Exp. Theor. Phys. (Engl. Transl.)*
[b] — *Dokl. Chem. (Engl. Transl.)*
[c] — *Quant. Electron. (Engl. Transl.)*
[d] — *J. Exp. Theor. Phys. Lett. (Engl. Transl.)*
[e] — *Nanotechnol. Russ. (Engl. Transl.)*
[f] — *Inorg. Mater.(Engl. Transl.)*
[g] — *Semiconductor (Engl. Transl.)*
[h] — *Phys. Solid. State (Engl. Transl.)*
[i] — *Colloid. J. (Engl. Transl.)*